

# Final Technical Report

**Award Number:** DE-EE0003496

**Project Title:** Research and Development of a New Silica-Alumina Based Cementitious Material Largely Using Coal Refuse for Mine Backfill, Mine Sealing and Waste Disposal Stabilization

**Project Period:** August 16, 2010 to March 31, 2012

**Recipient Organization:** University of the Pacific  
3601 Pacific Avenue, Stockton, CA 95211

**Author:** **Henghu Sun** (Principal Investigator)  
209-946-2767,  
Email: [hsun@pacific.edu](mailto:hsun@pacific.edu) ;

**Yuan Yao**  
209-946-7474  
Email: [y\\_yao@u.pacific.edu](mailto:y_yao@u.pacific.edu)

**Date of Report:** Jun 29, 2012

## **Acknowledgment**

This report is based upon work supported by the U. S. Department of Energy under Award No. DE-EE0003496.

## **Disclaimer**

Any findings, opinions, and conclusions or recommendations expressed in this report are those of the author(s) and do not necessarily reflect the views of the Department of Energy.

# Table of Contents

List of Acronyms	4
List of Tables	5
List of Figures	6
1. Executive Summary	7
2. Introduction	8
3. Background	10
4. Results and Discussion	13
4.1. <i>Raw Material Acquisitions</i>	13
4.2. <i>Improvement on Pozzolanic Reactivity of Coal Refuse by Thermal Activation</i>	14
4.3. <i>Durability Performance of Coal Refuse Based Silica Alumina Cementitious Material</i>	18
4.4. <i>A Novel Silica Alumina Based Backfill Material Composed of Coal Refuse and Fly ash</i>	26
5. Benefit Assessment	35
6. Commercialization	42
7. Accomplishments	43
8. Conclusions	44
9. Recommendations	45
10. References	45
11. Appendix (XRD Results and Interpretation)	47

## **List of Acronyms**

ASR	Alkali Silica Reaction
OPC	Ordinary Portland Cement
Btu	British Thermal Unit
CR	Coal Refuse
CCPs	Coal Combustion Byproducts
FGD Gypsum	Flue Gas Desulfurization Gypsum
XRD	X-ray Diffraction
XRF	X-ray Fluorescence
ASTM	The American Society for Testing and Materials
GU type cement	General Use Cement
W/C	Water to Cementitious Material Ratio
TCLP	Toxicity Characteristic Leaching Procedure
PRRC	Pacific Resources Research Center
SEC	Specific energy consumption

## Lists of Figures

3.1.	The flowchart of Project DE-EE0003496	12
4.2.1.	Compressive strength of mortar (Coal refuse:Cement=1:3) at 3 Days	15
4.2.2.	Compressive strength of mortar (Coal refuse:Cement=1:3) at 7 Days	15
4.2.3.	Compressive strength of mortar (Coal refuse:Cement=1:3) at 28 Days	16
4.2.4.	XRD results of coal refuse activated at different condition	16
4.3.1	The compressive strength test result (CR1 to CR3)	20
4.3.2.	Sorption plot of oven dried concrete mixes (CR1 to CR3)	21
4.3.3.	ASR mortar bar test result (CR1 to CR3)	22
4.3.4.	Stereo environment microscopy image of prismatic mortar sample surface at 16 aging day	22
4.3.5.	Temperature pattern of freezing-thawing test	23
4.3.6.	Freezing-thawing cabinet	24
4.3.7.	Samples of freezing-thawing test(CR1 to CR3)	24
4.3.8.	Relative dynamic modulus of elasticity of freezing-thawing test (CR1 toCR3)	24
4.3.9.	Rapid chloride permeability test results (CR1 toCR3)	25
4.4.1.	Particle Size distribution of the raw materials (coal refuse backfill)	27
4.4.2.	Flowability test of coal refuse and fly ash	28
4.4.3.	Scheme chart of the backfill material design (Coal refuse backfill)	28
4.4.4.	Performance of the backfill material	29
4.4.5.	Flowability test of backfill material Group B	31
4.4.6.	Compressive strength test of Backfill Material Group B4	32
5.1.	Energy consumption in cement production	36
5.2.	Energy consumption comparison between green cement and ordinary Portland cement	37
5.3.	On-site and primary energy consumption by cement making and green cement making in Process one	39
5.4.	Energy consumption summary of green cement production in process two	40
5.5.	CO <sub>2</sub> emission comparison between OPC and CRC	41

## List of Tables

4.2.1. Compositions of different tested groups	14
4.3.1. ASTM specifications followed in the experimental work	18
4.3.2. The recipe designs of different cementitious material (CR1 to CR3)	18
4.3.3. The laboratory mixture proportions of concrete test	19
4.3.4. Chemical composition ratio of four testing group (CR1 to CR3)	19
4.3.5. Key parameters of freezing-thawing test	23
4.3.6. Weight gained by high W/C ratio specimens during freezing-thawing cycles	23 28
4.4.1. Composition of backfill material group A	30
4.4.2. Composition of backfill material group B	31
4.4.3. Bleeding rates of B1-B5	33
4.4.4. TCLP results (Backfill body)	34
4.4.5. Technical index of the backfill technology	35
5.1. ASTM standards on the performance tests	35
5.2. Mixture composition of the cementitious material	36
5.3. Physical and Mechanical Performance of CRC and OPC	40
5.4. Relationship between specific surface and grinding time	

# 1. Executive Summary

Coal refuse and coal combustion byproducts as industrial solid waste stockpiles have become great threats to the environment. To activate coal refuse is one practical solution to recycle this huge amount of solid waste as substitute for Ordinary Portland Cement (OPC). The central goal of this project is to investigate and develop a new silica-alumina based cementitious material largely using coal refuse as a constituent that will be ideal for durable construction, mine backfill, mine sealing and waste disposal stabilization applications. This new material is an environment-friendly alternative to Ordinary Portland Cement. The main constituents of the new material are coal refuse and other coal wastes including coal sludge and coal combustion products (CCPs).

Compared with conventional cement production, successful development of this new technology could potentially save energy and reduce greenhouse gas emissions, recycle vast amount of coal wastes, and significantly reduce production cost. A systematic research has been conducted to seek for an optimal solution for enhancing pozzolanic reactivity of the relatively inert solid waste-coal refuse in order to improve the utilization efficiency and economic benefit as a construction and building material.

The results show that thermal activation temperature ranging from 20°C to 950°C significantly increases the workability and pozzolanic property of the coal refuse. The optimal activation condition is between 700°C to 800°C within a period of 30 to 60 minutes. Microanalysis illustrates that the improved pozzolanic reactivity contributes to the generated amorphous materials from parts of inert aluminosilicate minerals by destroying the crystalline structure during the thermal activation. In the coal refuse, kaolinite begins to transfer into metakaolin at 550°C, the chlorite minerals disappear at 750°C, and muscovite 2M<sub>1</sub> gradually dehydroxylates to muscovite HT (high temperature activated). Furthermore, this research examines the environmental acceptance and economic feasibility of this technology and found that this silica alumina-based cementitious material not only meets EPA requirements but also shows several advantages in industrial application. Compared with conventional cement production, successful development and commercialization of a new thermal activation process (500°C~900°C) to convert coal refuse into desirable pozzolanic material for producing the new material would potentially save energy around by about 54%, reduce greenhouse gas emissions by about 76%, recycle vast amounts of coal wastes, and significantly reduce production costs.

## 2. Introduction

Coal is still considered as the primary fuel for electricity generation (CTAB, 2010). However, the coal mining industry also generates a huge amount of inert solid waste during the mining process. Coal refuse is one of the largest forms of waste from the coal mining industry and is generally defined as a low BTU-value material under the parameters of minimum ash content combined with maximum heating value (Yao et al., 2012). It is estimated that coal mines in the US generate 109 million metric tons (120 million short tons) of coal refuse from 600 coal preparation plants in 21 coal-producing states annually. Such large quantities of the solid waste have not only occupied a great amount of land but also caused many serious environmental problems and the question of how to ecologically recycle the inert solid waste has become a very challenging topic and attracts the attention from the scientists and policy makers.

Coal refuse is a relative inert solid waste due to its major mineralogical compositions as stable aluminosilicate minerals at the ambient conditions, such as quartz, feldspar etc., which is hard to utilize as cementitious material for its lack of pozzolanic properties. In this project, a systematic study was conducted on evaluating the enhanced pozzolanic property of a coal refuse based silica alumina cementitious material which is generated by thermal activation. A detailed microanalysis was performed to illustrate the mineral phase change and morphological modification of coal refuse during the thermal activation process.

Developing sustainable production techniques in the cement industry is a top environmental priority. Conventional Ordinary Portland Cement (“OPC”) production has been a leading contributor to problems such as energy depletion, resource exhaustion, and severe pollution of the environment - all roadblocks to continued sustainable development. OPC production pollutes in a variety of ways, but most conspicuously in its emission of carbon dioxide. OPC accounts for 6% of the world’s greenhouse gases, an 8 fold increase globally since the mid 1960’s. The manufacturing process depends on burning vast amounts of coal to heat kilns normally to more than 1,450 °C. It also relies on the decomposition of limestone, a chemical reaction which releases carbon dioxide as a byproduct. Lime, or calcium oxide (CaO), is created by heating calcium carbonate (CaCO<sub>3</sub>) in large furnaces called kilns. The process of heating calcium carbonate to yield lime is called “calcination” or “calcining” and is written chemically as:  $\text{CaCO}_3 + \text{Heat} \text{ yields } \text{CaO} + \text{CO}_2$ . In this chemical reaction, 0.534 tons of CO<sub>2</sub> per ton of cement is produced, and approximately another 0.4 tons of CO<sub>2</sub> per ton of cement is produced through the emissions from fossil fuels used to drive this reaction. Cement plants in the whole world are projected to emit almost 5 billion tons of CO<sub>2</sub> annually by 2050.

In U.S, OPC consumes 400 trillion Btu of energy and emits 82 million metric tons of carbon dioxide per year. OPC production involves two grinding stages and one calcination stage (heating at 1200°C to 1540°C). Based on 1999 national statistics, for OPC production, the total specific energy consumption (SEC) is 4.1 MBtu/ton (0.50 MBtu/ton for electricity SEC and 3.9 MBtu for fuel SEC).

Silica-alumina based cementitious material is an environmentally friendly alternative to Ordinary Portland Cement. In contrast to OPC production, the manufacturing of silica-alumina based cementitious material does not require a high temperature calcination process but uses a lower

temperature thermal activation process at an optimal temperature ranging between 500°C to 800°C. Based on thermal heating guidelines, maintaining a temperature between 500°C and 800°C would require a maximum 20% to 33% (on average 25%) of the energy needed to maintaining a temperature between 1200°C and 1540°C. Moreover, in terms of electricity expenditure, since only one grinding process is required, a further savings in energy can be made. At the same time, the thermal activation process at the temperature 500°C to 800°C does not decompose the  $\text{CaCO}_3$  and it can significantly reduce the  $\text{CO}_2$  emission.

This project was a TRL 1 research stage which provided the scientific feasibility of a technology for future commercialization to improve the energy efficiency and reduce the greenhouse gas emission but it does not contain any approaches or planning for future commercialization.

### 3. Background

Industries such as power generation, coal mining, steel production and chemical production create vast amounts of solid wastes which pollute into the environment. These kinds of silica-alumina rich coal mining wastes can be mixed together in appropriate proportion along with cement and flue gas desulfurization (FGD) gypsum, to produce a high performance silica-alumina based cementitious material, significantly reducing the need for OPC. The main manufacturing process of the silica-alumina cementitious material production would use industrial waste materials with pozzolanic properties as raw material, which would require relative lower temperature (700 °C to 800 °C) compared to the OPC production (1200°C to 1540°C), with generating much less carbon dioxide or other greenhouse gases. Through investigation of the silica-alumina cementitious material's application in various laboratory tests and industrial settings using a variety of waste inputs, we plan to achieve performance requirements that result in a silica-alumina based cementitious material by using coal refuse and CCPs that meets the current OPC industry standards.

Before describing the silica-alumina cementitious material in more detail and explaining the initial research that led to its creation with blast furnace slag, it is important to establish that the silica-alumina cementitious material is not merely an extension of the vast amount of research that has already been conducted on alkali slag cement and geopolymer cement. The silica-alumina cementitious material is, in fact, a new cementitious material with fundamentally different hydration products.

In recent decades, the study on alkali slag cement has made great progress in other countries and broken through the content restriction of alkali metal oxides ( $R_2O$ ) required by the traditional Portland cement standards with excellent performance similar to “Geopolymeric Cement” (Davidovits, J. 2008). However, due to the high costs of raw materials and difficult implementation, the use of alkali slag cement has not been adopted on a large-scale. And it is necessary to produce silica-alumina based cementitious material with low-cost, high-performance, environment-friendly characteristics using a variety of industrial solid wastes (such as fly ash, metallurgical slag, tailings and coal refuse). Whereas OPC is made with over 80% clinker dosage, silica-alumina based cementitious material is transformative in that it requires as low as less than 30% clinker dosage. Considering current OPC standards, certain amount of clinker dosage (about 30%-70%) in the silica-alumina based cementitious material may be required for research in the project.

The central goal of this project was to investigate and develop a new silica-alumina based cementitious material largely using coal refuse as a constituent that will be ideal for mine backfill, mine sealing and waste disposal stabilization applications. This new material is an environment-friendly alternative to Ordinary Portland Cement. The main constituent of the new

material will be fine coal refuse and coal wastes, including coal sludge, coal combustion products (CCPs) and other related wastes in the coal mining industry. Most of these materials end up loosely stockpiled in coal waste deposits throughout the country and, consequently, threaten the surrounding biosphere.

Compared with conventional cement production, successful development and commercialization of this new technology could potentially save energy by about 60% and reduce CO<sub>2</sub> by about 80%, recycle vast amount of coal wastes, and significantly reduce production cost. The research had the following four objectives:

1. Create a new silica-alumina based cementitious material which meets or exceeds the requirements applied to Portland cement for the same application.
2. Design a thermal activation process (500°C~800°C) to convert coal refuse into desirable pozzolanic material for producing the new material, which is more energy-efficient and environment-friendly than the process used for manufacturing cement.
3. Develop new materials for mine backfill, mine sealing and waste disposal stabilization using the new cementitious material as binder.
4. Demonstrate using a laboratory scale model that the production of the new material will lead to significant reduction in energy consumption by about 54% and CO<sub>2</sub> emission reduction by about 76% with respect to Portland cement production.

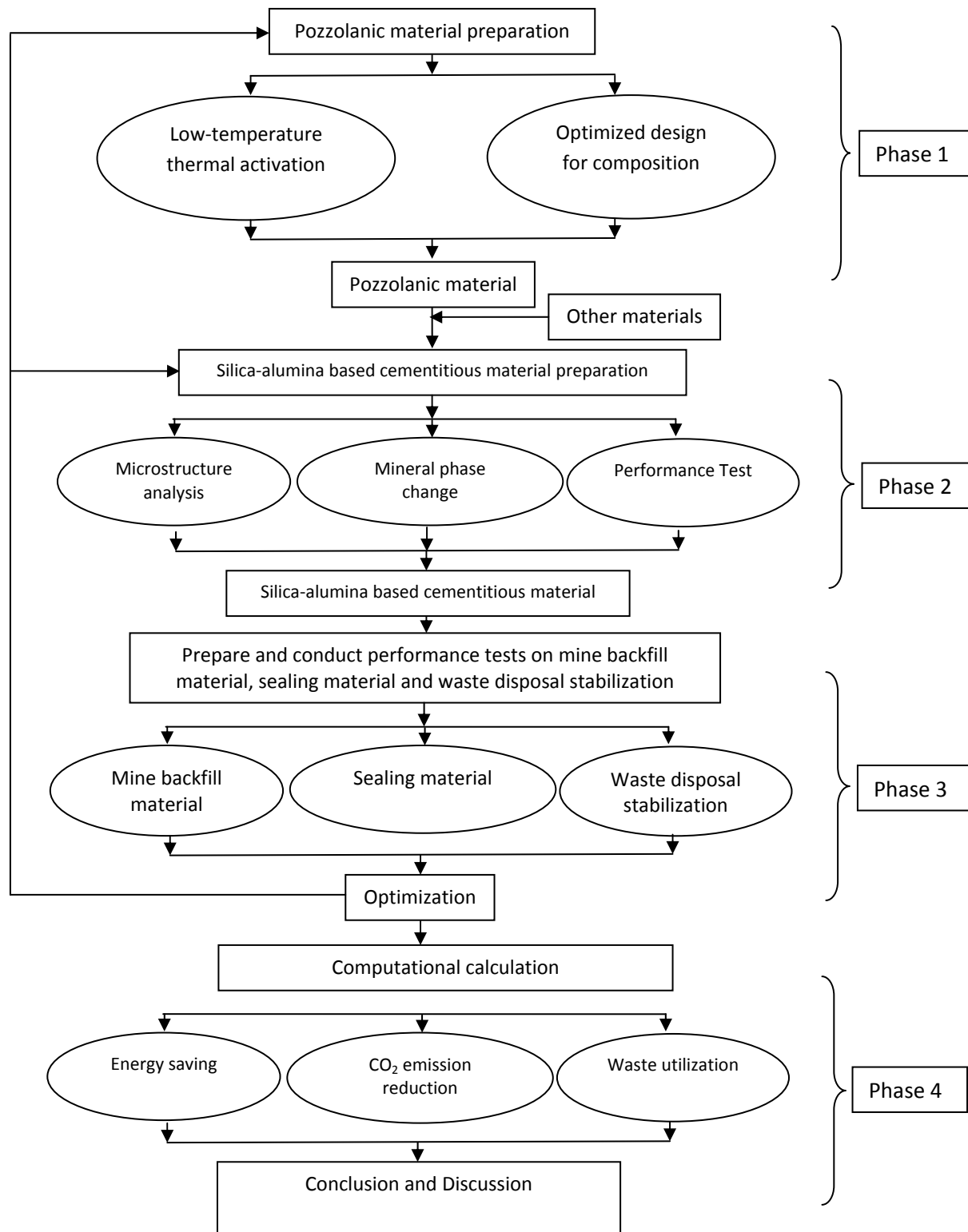


Figure 3.1 The flowchart of Project DE-EE0003496

## **4. Results and Discussion**

### **4.1. Raw Material Acquisitions**

Raw material acquisitions were accomplished through Silica Alumina LLC's support. Coal refuse, coal sludge, and coal combustion products (CCPs) were from coal mines and coal power plant from Arch Coal, West Virginia. CCPs include fly ash and bottom ash which are from Tennessee Valley Authority (TVA), Tennessee, and the iron slag which is from Lehigh, California. Other materials including water reducer, superplastizer, limestone, dolomite and garden gypsum and flue gas desulfurization (FGD) gypsum were collected directly by PRRC (Pacific Resources Research Center) team. Material characterization which includes physical and chemical analysis was accomplished through collaboration with UC Davis, UC Riverside and UC Berkeley. X-ray Diffraction (XRD), X-ray Fluorescence (XRF), Scanning Electron Microscope (SEM), and Laser Particle Size Analyzer (LPSA), specific surface and gravity analyses were applied for the raw materials characterization. The appendix provides XRD results and data interpretation. For the cementitious material development, all the raw material was necessary to be grounded into fine powders.

## 4.2. Improvements on Pozzolanic Reactivity of Coal Refuse by Thermal Activation

### 4.2.1. Pozzolanic properties of coal refuse.

The compressive strength test was used to evaluate the pozzolanic properties of the coal refuse based cementitious material. Cubic specimens (50 mm × 50 mm × 50 mm) were cast for each mixture for the unconfined compressive strength test (ASTM C109, 2008). According to recipe of coal refuse based cementitious material (CR) in table 4.2.1, the coal refuse activated at different condition and were mixed respectively to form different cementitious material groups.

The compressive strength results are presented in figures 4.2.1, 4.2.2 and 4.2.3. It is clearly seen that the 3 day strength of all coal refuse based cementitious material reaches more than 27 MPa. The 3 days strength of samples activated at 700 °C and 800 °C is higher than 28 MPa which is slightly better than that of Ordinary Portland Cement (OPC) group. When compared with the groups activated at different temperature, it is found that the groups with 1 h and 1.5 h activation show better pozzolanic property than the group with 0.5h activation. As for the 7 and 28 day strength performance, it is also found the similar phenomenon which shows that the 7 day strength of group activated at 700 °C for 1 h reaches to 36.8 MPa, and it is higher than other groups in the 7 day strength test.

Table 4.2.1 Compositions of different tested groups

Sample	Cementitious materials(kg/m <sup>3</sup> )		Sand (kg/m <sup>3</sup> )	Water (kg/m <sup>3</sup> )	W/C	S/C
	Cement	Pozzolana				
OPC	500	0	1375	242	0.485	2.75
CR	375	125	1375	242	0.485	2.75

(Pozzolana= coal refuse + gypsum at 20:1 ratio)

In the 28 Day strength test, the strength of groups with 700 °C 1h activation and 800 °C 1h activation reaches 43.4MPa and 43.1 MPa respectively, which is higher than the 40 MPa strength of OPC at 28 days. From these three sets of strength tests at different curing age, it can be concluded that the activation temperature from 700 °C to 800 °C usually shows better activation performance than the activation at 500° C to 600°C when the process was conducted at the same time duration. And as for the same temperature activation condition, 1 h and 1.5 h activation shows better effect than activation within 0.5 h.

Therefore, the optimal activation temperature for the coal refuse is from 700 °C to 800 °C, and the optimal time is 0.5 hour to 1hour.

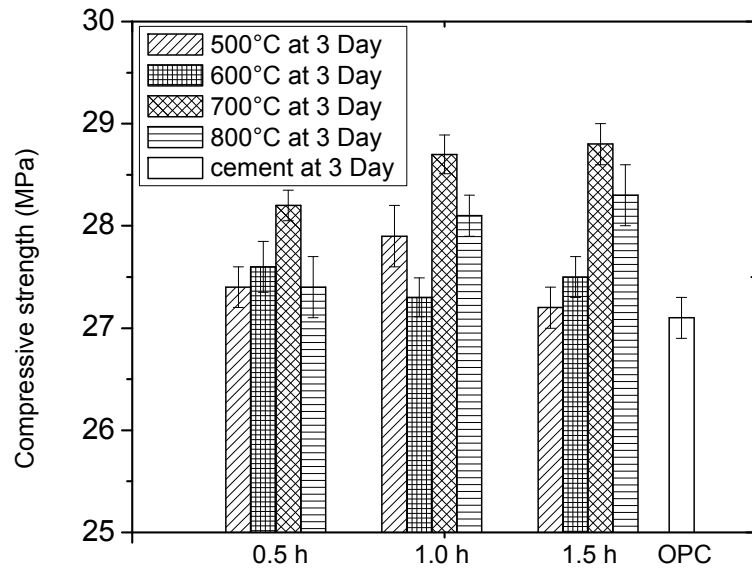


Figure 4.2.1 Compressive strength of mortar (Coal refuse:Cement=1:3) at 3 Days

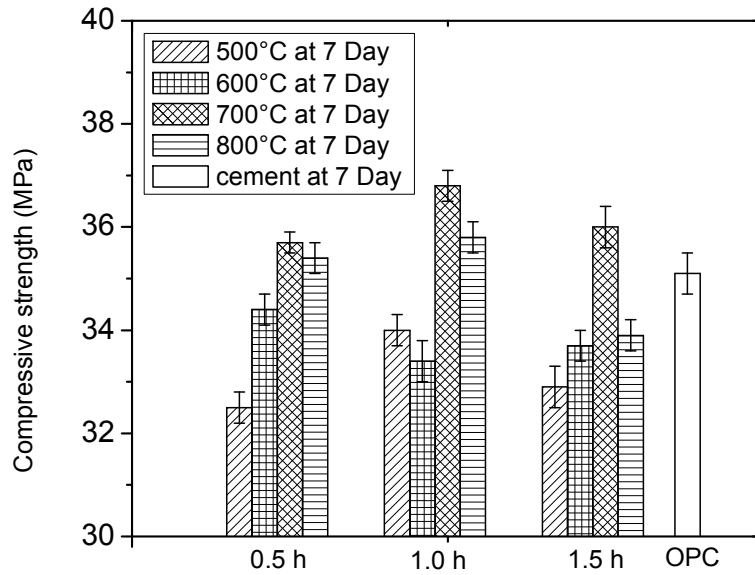


Figure 4.2.2 Compressive strength of mortar (Coal refuse: Cement =1:3) at 7 Days

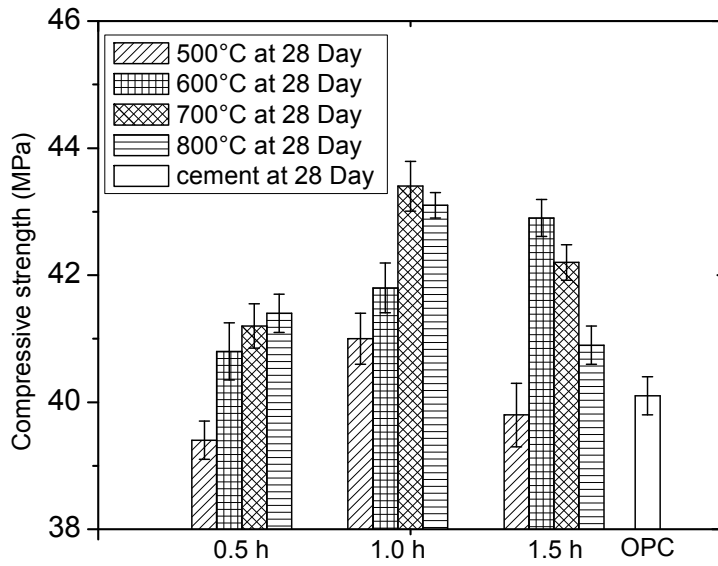


Figure 4.2.3 Compressive strength of mortar (Coal refuse: Cement= 1:3) at 28 Days

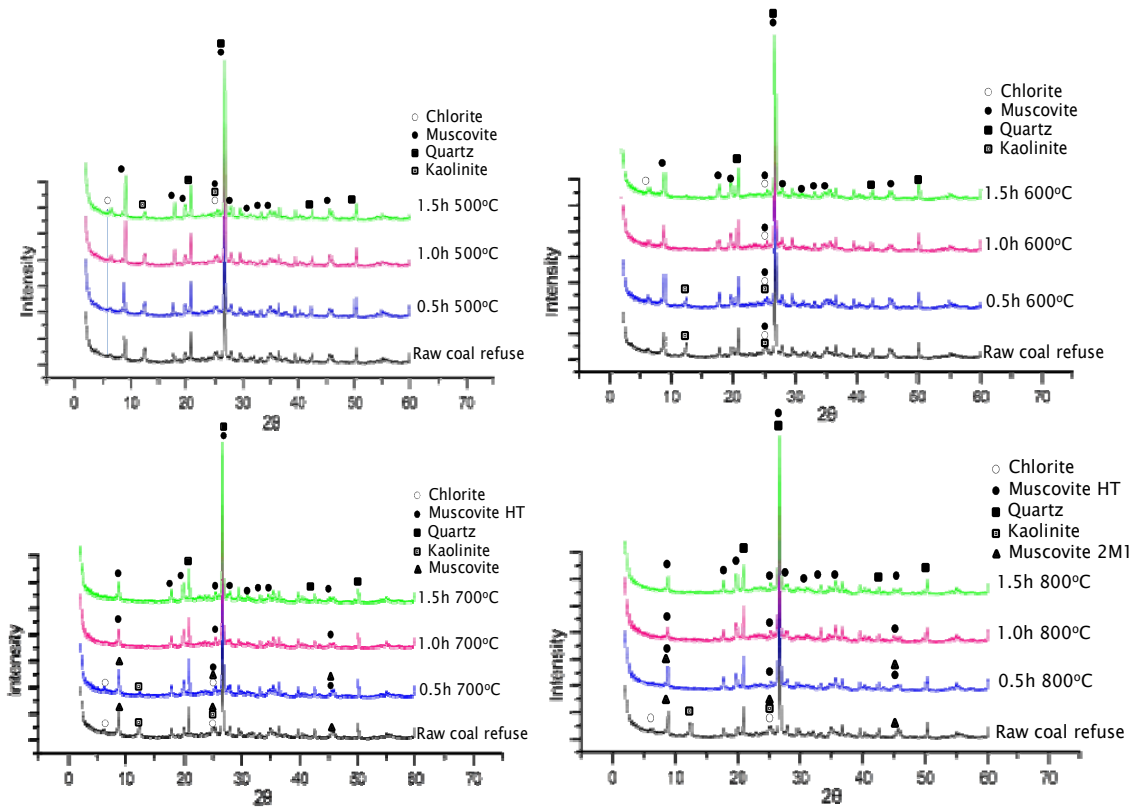
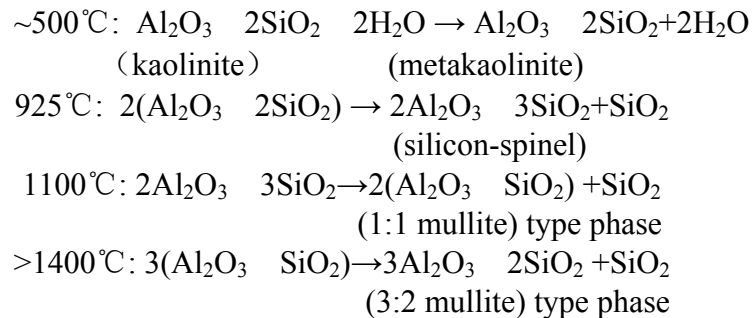


Figure 4.2.4 XRD results of coal refuse activated at different condition

Figure 4.2.4 shows that the mineral phase change for coal refuse was significant. It is obvious that the peaks assigned to kaolinite and muscovite disappeared at 600°C to 800°C, and the peaks associated with quartz were obviously decreased at 800°C. The kaolinite as well as chlorite peaks began to decrease because of their transformation into metakaolin at 600°C to 800°C, while the muscovite peaks decreased at 700°C, which may have been caused by the decomposition of muscovite to form some amorphous silicon-based material. Muscovite amorphizes at high temperature and high pressure; muscovite 2M<sub>1</sub> shows a major phase transition at about 800°C and the reaction taking in 700°C to 1000°C is truly a dehydroxylation process, involving the muscovite 2M<sub>1</sub> gradually dehydroxylated to muscovite HT (Yao et al., 2012). The generated amorphous materials from parts of decomposed inert aluminosilicate minerals might be contributing to the improved pozzolanic properties, other observations are:

1. The kaolinite peaks began to decrease because of their transformation into metakaolin at 550°C, and the kaolinite peaks disappeared at 750°C.
2. Chlorite peaks began decreasing at 550°C and disappeared at 750°C.
3. Muscovite peaks decreased at 750°C and disappeared at 950°C.
4. At 950°C, the quartz peak was weakened by the thermal activation and may have been caused by the decomposition of clay minerals that formed amorphous silicon-based material.
5. The hematite peaks in XRD spectra becomes more evident after thermal activation, especially at 950°C.
6. Calcite peaks decreased but still exist when the temperature rise up to 950°C, which might due to the decomposition of the calcite (Zhang et al., 2012).

And the chemical reaction are:



For further detailed discussion on the mineral transformation, please refer to “Y.Yao, H.Sun. (2012). A novel silica alumina-based backfill material composed of coal refuse and fly ash. *Journal of Hazardous Materials*. 213-214:71-82.”

### 4.3. Durability Performance of Coal Refuse Based Silica Alumina Cementitious Material

#### 4.3.1. Durability test procedures.

All performance tests were performed according to the provisions of the relevant ASTM standards. The various tests and relevant ASTM standards followed in this experimental program are given in table 4.3.1. The recipe designs of different cementitious materials and the mixture proportions of concrete test are described in tables 4.3.2 and 4.3.3, respectively. Table 4.3.4 list the chemical composition of different cementitious material recipe (CR1 to CR3)

Table 4.3.1 ASTM specifications followed in the experimental work

Test description	Specification
Concrete mixing and curing	ASTM C192
Compressive strength	ASTM C39, ASTM C109
Flowability (Slump)	ASTM C143
Density(Fresh concrete)	ASTM C138
Density(hardened concrete)	ASTM C642
Sorption	ASTM C1585
Chloride ion penetration	ASTM C1202
Freezing-thawing resistance	ASTM C666
Alkali-silica reaction	ASTM C1260

Table 4.3.2 The recipe designs of different cementitious material (CR1 toCR3)

Testing group	Type I/II cement (%)	Gypsum (%)	Pozzolanic material (%)
Cement	100	0	0
CR1	65.1	2.5	30
CR2	45.5	2.5	50
CR3	27.9	2.1	70

(Pozzolanic material= Coal refuse+ Slag at 1:1 Ratio)

Table 4.3.3 The laboratory mixture proportions of concrete test

Cementitious Material (w/w %)	Gravel (w/w %)	Sand (w/w %)	Water (w/w %)
19.8%	49.8%	21.3%	9.1%

Table 4.3.4 Chemical composition ration of four testing group (CR1 to CR3)

	CaO(%)	SiO <sub>2</sub> (%)	Al <sub>2</sub> O <sub>3</sub> (%)	SO <sub>3</sub> (%)	Fe <sub>2</sub> O <sub>3</sub> (%)	Ca/Si	Ca/Al	Si/Al	C <sub>3</sub> A
Cement	68.89	16.99	3.78	2.54	3.34	4.05	18.22	4.49	4.36
CR1	53.18	23.04	6.64	3.33	4.11	2.31	8.01	3.47	10.63
CR2	44.53	27.69	8.68	3.05	4.75	1.61	5.13	3.19	14.96
CR3	37.09	32.68	10.79	2.61	5.45	1.14	3.44	3.03	19.38

Note: C<sub>3</sub>A= 3 CaO • Al<sub>2</sub>O<sub>3</sub>

#### 4.3.2. Mechanical properties.

Based on the previous study, coal refuse activated at 750 °C has been concluded to yield better pozzolanic property when compared with those activated from 150°C to 950°C for the same time duration. In this case, the pozzolana is determined to be a mixture of coal refuse (activated at 750 °C for 1 hour) and blast furnace slag at a fixed 1:1 ratio. The mechanical strength test results are shown in figure 4.3.1. When comparing the strength properties from CR1 to CR3, CR1 has higher strength values than CR2 and CR3 at each specific curing age. This difference might be largely due to the higher CaO content in the CR1 group rather than those of CR2 and CR3. From CR1 to CR3, the trend of the CaO content, SO<sub>3</sub> content, Ca/Si, Ca/Al and Si/Al is decreasing, whereas that of SiO<sub>2</sub> and Al<sub>2</sub>O<sub>3</sub> is increasing (table 4.4.4). These trends correspond well with the mechanical property change pattern in the compressive strength test. In geopolymer research, the effect of calcium has been recently investigated, and the amount of Ca in the raw materials and the form in which it is present both play significant roles in determining the reaction pathway and physical properties of the final hydration products (Davidovits, J. 2008). Although there is no alkali solution directly mixed with the cementitious material to form geopolymers in this experiment, the alkali microenvironment of hydration reaction, especially the cement hydration portion of each testing group, still provide a large potential for polymerization during the entire process. Therefore, in this experiment, the addition of a sufficient quantity of Ca to the cement and CR1 can lead to the formation of a calcium silicate hydrate (C-S-H) gel and/or phase-separated Al-substitute calcium silicate hydrate (C-(A)-S-H).

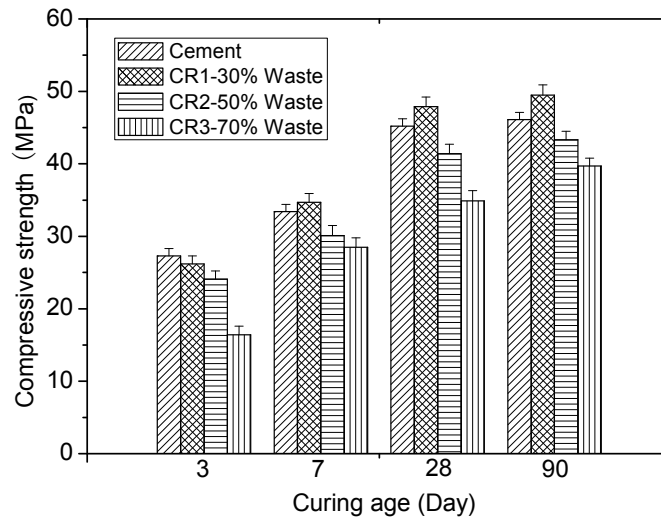


Figure 4.3.1 The compressive strength test result (CR1 to CR3)

#### 4.3.3. Sorption test.

The entry of moisture into a porous concrete structure is one of the most common physical phenomena and causes damage to the physical properties and microstructure of the concrete. These sorption tests were performed in accordance with ASTM C 1585. The corresponding sorption plots of the four test groups are shown in figure 4.3.2. A higher pozzolana amount has a higher water sorption value when compared with the cement control mix.

#### 4.3.4. Alkali-silica reaction test.

The alkali-silica reaction (ASR) occurs between certain aggregates and the highly alkaline pore fluids in cement paste. The reaction will form a gel-like product, which expands in the presence of water and may cause the cracking of mortars or concretes. In this project, three different recipes of coal refuse-based cementitious material were designed for casting prismatic specimens that were tested for alkali-silica reactions in accordance with ASTM C 1260 and ASTM C 1567 (ASTM C 1260, 2008, ASTM C 1567, 2008). For each 25×25×285mm prismatic mortar bar mix, a fixed cement-to-fine aggregate ratio of 1:2.25 was used. After the casting, the prismatic mortar bars were aged in a sodium hydroxide (NaOH) solution at 80°C continuously for 28 days with intermittent readings of the length change of the bars taken during the course of the test. ASR-related expansions less than 0.10% at 16 days after casting are indicative of innocuous behavior, while those between 0.10% and 0.20% at the same age are indicative of both innocuous and deleterious behavior in field performance; expansion greater than 0.20% at 16 days of age are indicative of potentially deleterious expansion.

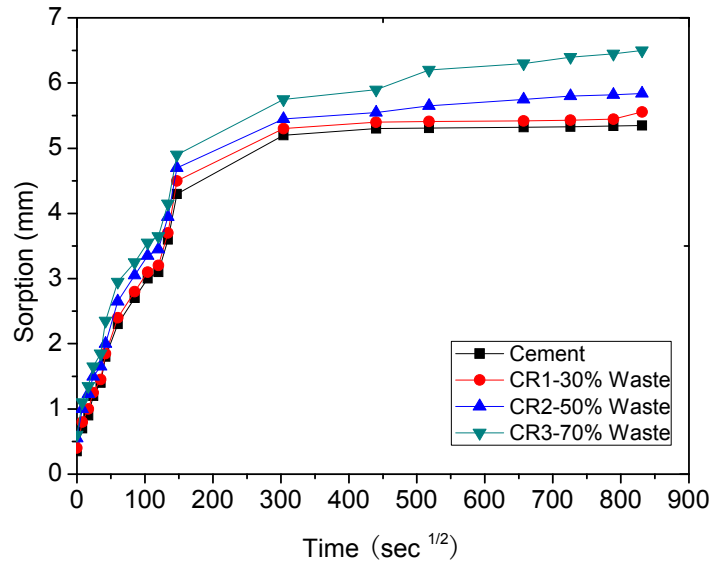


Figure 4.3.2 Sorption plot of oven dried concrete mixes (CR1 to CR3)

The ASR test showed that the expansion development is 0.16% at 16 days and 0.18% at 28 days, indicating the potential deleterious behavior of the cement group (figure 4.3.3). In contrast, none of the other three groups (CR1 to CR3) exceeds the 0.10% limitation, indicating the innocuous behavior of these three groups. The increasing amount of pozzolana material (mixed coal refuse and slag) as a substitute for the OPC cement reduced the ASR expansion, and the 16-day expansion rate of CR2 and CR3 is only 0.04% and 0.028%, respectively. Therefore, the application of pozzolana material as a substitute for OPC cement will significantly reduce the potential damage cause by ASR. Stereo environment microscopy illustrates the cracking on the tested samples cause by ASR (figure 4.3.4), with the cement group clearly having more pronounced cracking than the three other groups containing the pozzolana substitute, which corroborates the results in figure 4.3.4.

Over the past decade, there have been a great number of studies that discuss the resistance of blended cement to the alkali silica reaction. Generally, the swelling phenomenon can be considered to be induced by the formation of an ASR gel at the interface between the aggregate and cement paste. The chemical mechanism can be generally written as the following main steps: (Chatterji et al., 2000)

1.  $2\text{SiO}_2 + \text{OH}^- \rightarrow \text{SiO}^-_{5/2} + \text{SiO}_{5/2}\text{H}$
2.  $\text{SiO}^-_{5/2} + \text{OH}^- + 1/2 \text{H}_2\text{O} \rightarrow \text{H}_2\text{SiO}_4^{2-}$
3.  $\text{H}_2\text{SiO}_4^{2-} + \text{Ca}^{2+} + x\text{H}_2\text{O} \rightarrow \text{C-S-H}$
4.  $\text{H}_2\text{SiO}_4^{2-} + \text{Ca}^{2+} + 2\text{M}^{2+} + y\text{H}_2\text{O} \rightarrow \text{C-M-S-H}$  (M can be K, Mg or other alkali element)

From (3) and (4),  $\text{Ca}^{2+}$  and alkalinity can be inferred to determine the chemical reaction speed. Therefore, the higher  $\text{Ca}^{2+}$  concentration and alkalinity yield the more serious ASR reactions in cement. In contrast, the pozzolana-blended cementitious material in CR1 to CR3 shows much lower ASR reactions. In our test, the CaO content decreased from 68.89% in cement to 37.37% in CR3, and the Ca/Si also decreased from 4.05 in cement to 1.14 in CR3 (Table 4.4.4).

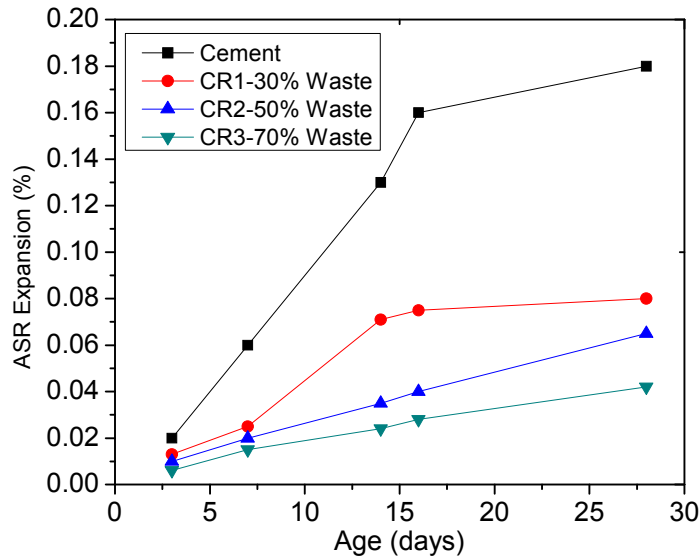


Figure 4.3.3 ASR mortar bar test result (CR1 to CR3)

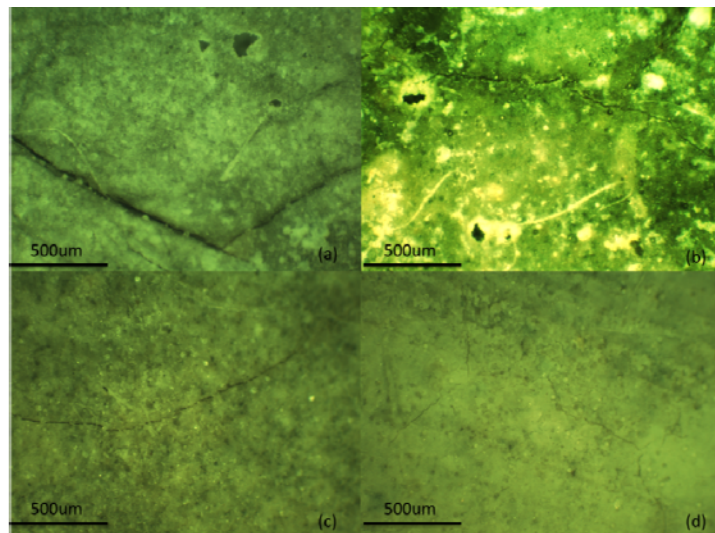


Figure 4.3.4 Stereo environment microscopy image of prismatic mortar sample surface at 16 aging day: (a). cement; (b). CR1; (c). CR2; (d) CR3.

### 4.3.5. Freezing-thawing tests.

The freezing-thawing tests were performed as described in ASTM C666 (parameters given in Table 4.3.5). The concrete beams were subjected to 300 freezing-thawing cycles, and the visual appearance of the four groups varies significantly (Figure 4.3.6). The surfaces of the cement and CR1 samples were still in good condition, while that of CR2 was slightly damaged. In contrast, CR3 had a gloomy and coarse surface, on which nearly half of its original surface cover had a flaking problem.

Increased weight due to water absorption is an indication of the extent of deterioration of the concrete due to interior cracking under the freezing-thawing cycles. The weight gain for each of the concrete materials is shown in Table 4.3.6. The increasing amount of pozzolana yield corresponded with increasing weight gains, from the CR1 value of 0.42 % to the CR3 value of 0.59 %. The cement has the lowest value at 0.35 %.

Table 4.3.5 Key parameters of Freezing-thawing Test

Temperature Range	Freezing rate	Cycle rate	Freezing Hour /Cycle	Thaw Hour /Cycle
4 °C to -18 °C (40 °F to 0 °F)	18 °C/h (51.8 °F/h)	8 cycle/24h	2	1

Table 4.3.6 Weight change by high W/C ratio specimens during freezing-thawing cycles

Mix designs	Cement	CR1	CR2	CR3
Weight change (%)	0.35	0.42	0.48	0.59

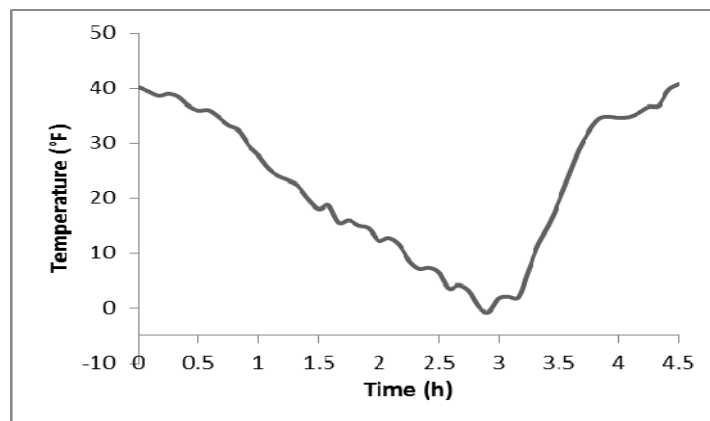


Figure 4.3.5 Temperature pattern of Freezing-thawing test



Figure 4.3.6. Freezing-thawing cabinet      Figure 4.3.7. Samples of freezing-thawing test  
(Left to right: Cement; CR1; CR2; CR3)

The changes in concrete beam relative dynamic modulus of elasticity correspond well with the visual appearance and weight variation seen in the freezing-thawing test. The variation of relative dynamic modulus of elasticity of cement and CR1 has a very close trend, with the final values of relative dynamic modulus of elasticity as 91.2% and 91.0%, respectively (Figure 4.3.8). Although the relative dynamic modulus of elasticity of CR2 remained at 61.5% for the full 300 cycles, this value is much lower than those for cement and CR1. The relative dynamic modulus of elasticity of CR3, however, dropped below 60% at approximately 180 cycles, which indicates the serious inner microstructure damage caused by the water penetrating the whole concrete structure. In this case, the optimal group in the freezing-thawing test is CR1.

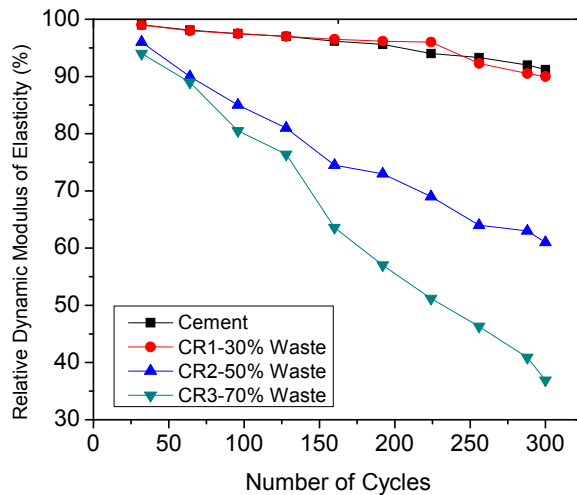


Figure 4.3.8 Relative dynamic modulus of elasticity of freezing-thawing test (CR1 to CR3)

In this test, the assessment of the frost soundness of pozzolanic material-based concrete requires special consideration due to the highly water absorptive nature of coal refuse. The increasing amount of the coal refuse mixed in the cementitious material enhanced the water absorption of the cementitious material, as shown by the weight measurements in Table 4.3.6. Although all four tested groups have exactly the same aggregates and water content, the CR3 with more pozzolanic material will absorb more water than will CR1 and CR2. This large amount of water distributed in the matrix of the cementitious material might cause significant volume changes between the cementitious material and aggregate, thus causing the interior structure damage represented by the great decrease in the dynamic modulus of CR3 shown in Figure 4.3.8.

#### 4.3.6. Chloride permeability test.

The chloride permeability test involves monitoring the amount of electrical current (coulombs) passed through a 102-mm diameter by 51-mm thick concrete disc with a potential difference of 60 V DC maintained across the specimen for a period of 6 h. Chloride ions are forced to migrate out of a NaCl solution subjected to a negative charge through the concrete into a NaOH solution maintained at a positive potential. According to ASTM C1202, if the number of coulombs passed lies between 2000 and 4000, the chloride permeability of concrete is considered low, and it is considered very low for the 100-1000 range. The increasing amount of pozzolana enhances the chloride penetration resistance, with the number of coulombs passed through CR2 and CR3 below 1000, which is considered to be very low (Figure 4.3.9). Although the number of coulombs passed through CR1 is 1298, it is much lower than that of the cement group.

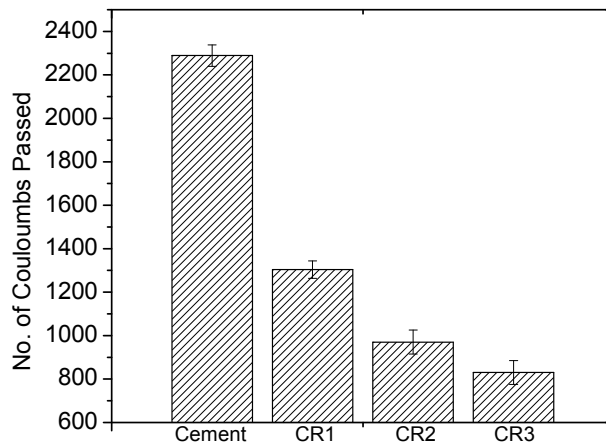


Figure 4.3.9 Rapid chloride permeability test results (CR1 to CR3)

## **4.4. A Novel Silica Alumina-Based Backfill Material Composed of Coal Refuse and Fly Ash**

### **4.4.1. Backfill material introduction**

Backfill refers to any waste material that is placed in voids mined underground for the purpose of either disposal or performing engineering functions. The backfill industry is particularly interested in technologies that reduce the costs associated with backfilling large open stopes. In this project, a systematic study was conducted on a novel, high-performance, silica alumina-based backfill material, which was designed by taking advantage of the pozzolanic property of thermal activated coal refuse and the good flowability of fly ash. Furthermore, a detailed microanalysis was performed to illustrate the mechanism of coal refuse thermal activation and environmental leaching. The results (Yao.Y and Sun. H, 2012) proved the environmental acceptance of this new backfill material.

### **4.4.2. Experimental Procedure**

ACI 229 report, ASTM D6103 was used to evaluate the consistency of the controlled low strength material (ACI 229R, 1999). For the compressive strength test, 50 mm × 50 mm × 50 mm cube specimens were cast for each mixture. The compression tests were performed on six specimens of various ages (1, 3, 7, 28, 56, 90 days). A high bleeding rate is often observed in fly ash-based cementitious material because of the spherical shape of the fly ash particle. In this test, as described in ASTM C 232, the water bleeding rate was measured according to the amount of water accumulated at different time intervals on the sample surface of an approximately 14 liter cylindrical container with an inside diameter of  $255 \pm 5$  mm and a height of  $280 \pm 5$  mm (ASTM C232, 2008).

The raw coal refuse used in the experiments was an irregular, rock-like stone with a large size range from 1 mm to 30 cm. The raw coal refuse was divided into two categories: coarse coal refuse as aggregate and coal refuse after milling as pozzolanic material with a specific surface area of  $564 \text{ m}^2/\text{kg}$  measured using the Blaine method. As was the case for the raw fly ash, the particle size was smaller than that of the raw coal refuse, and the fly ash after milling had a specific area of  $551 \text{ m}^2/\text{kg}$ . The industrial commercial slag, cement and FGD gypsum were in a fine powder state, with high Blaine values. The aggregate was a mixture of different ashes, particles and stones. Figure 4.4.1 illustrates the particle distribution of the raw materials. Except for the coal refuse aggregate, all of the raw material fell into the range of 1-6  $\mu\text{m}$ , and more than 80% of the particles were less than 2  $\mu\text{m}$ . Most of the coal refuse aggregate ranged from 1 mm to 16 mm in diameter, with the highest frequency distribution being 1-4 mm; however, there were still some large particle size distributions in the aggregate, such as 7% at 12 mm, 1% at 14 mm

and 1% at 16 mm. All of the raw material was below 19 mm, which meets the ASTM D6103 standard (ASTM D6103, 2008).

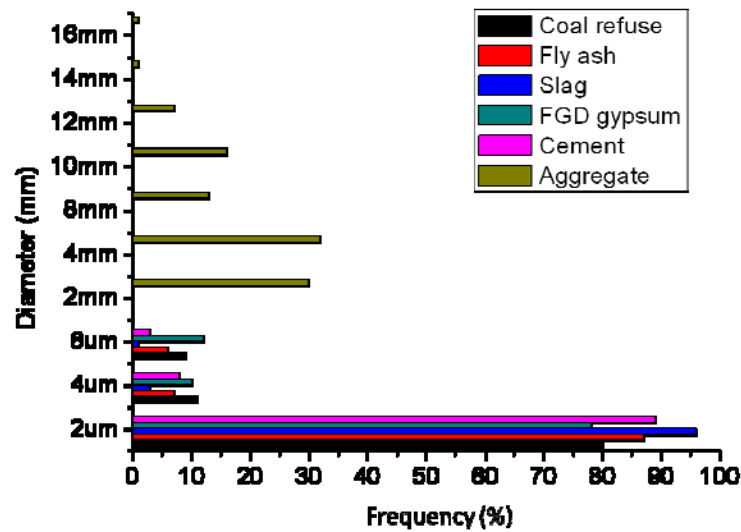


Figure 4.4.1 Particle size distribution of the raw materials (Coal refuse Backfill)

#### 4.4.3. Flowability test for the coal refuse and fly ash.

Figure 4.4.2 clearly shows that the fly ash has better flowability than the coal refuse when they have the same water/solid (W/S) ratio. For example, when the W/S was 0.4, the spread diameter for the 20°C coal refuse was only 94 mm, whereas that of the 20°C fly ash was 265 mm. This result is due to the spherical shape of the fly ash ball, which behaves as a non-Newtonian fluid with a low permeability coefficient that reduces pipeline wear (the cylinder wall in this experiment). On the other hand, the coal refuse after milling is an irregular particle, which is more abrasive to the cylinder wall. However, it is interesting to note that the thermal activation of the coal refuse increased its flowability; however, the thermal activation did not notably improve the flowability of the fly ash. Furthermore, when the temperature was increased to more than 750°C, the 750°C activated fly ash powder showed an agglomeration phenomenon that was more intense than that of the 750°C activated coal refuse. Therefore, there was a decreasing tendency in the flowability at temperatures between 550°C and 950°C for the fly ash. However, the total flowability of the coal refuse increased at temperatures of 20°C to 950°C.

#### 4.4.4. Performance of the backfill material.

Generally, the backfill material contained different categories of raw material, including water, cementitious material, aggregates and others. The variation in the composition of the backfill material significantly influenced its performance. To obtain the performance characteristics of the backfill material, it is necessary to evaluate the flowability of the fresh backfill slurry and the compressive strength of the hardened body at different pulp densities (the amount of solid

material of the total backfill material). Table 4.4.1 and Figure 4.4.3 present the composition and design scheme of the tested backfill material in this experiment. Generally, the solid part of this backfill material is divided into three categories: cementitious material (cement+slag+FGD gypsum), activated material (coal refuse or fly ash) and aggregates.

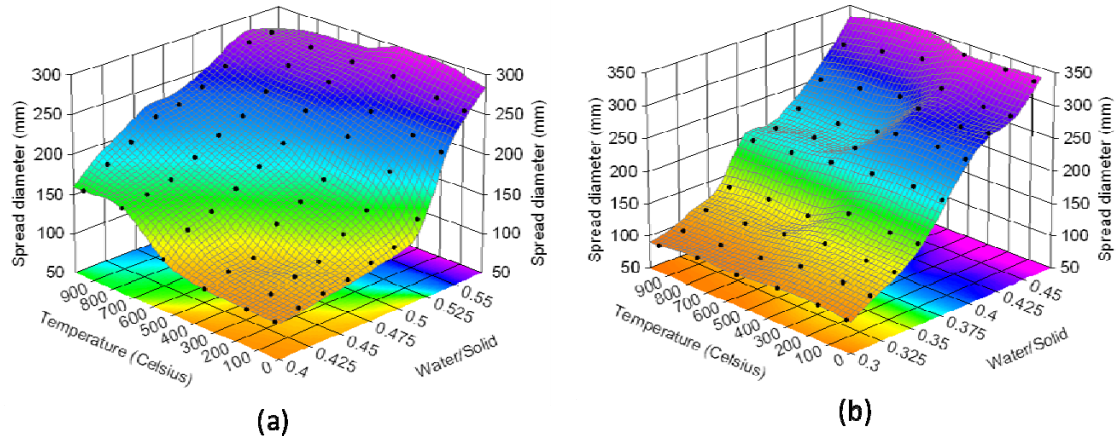


Figure 4.4.2 Flowability test of coal refuse and fly ash: (a) Coal refuse; (b) Fly ash  
(Each black point on figure 2 represents the mean of 6 replicates at one recipe design, and none of the standard deviation in each recipe design is larger than 3)

Table 4.4.1 Composition of Backfill Material Group A

	Binder			Activated material		Aggregate
	Cement	Slag	FGD gypsum	Coal refuse	Fly ash	Coarse refuse
A1% (w/w)	1	1	1	20	0	77
A2% (w/w)	1	1	1	0	20	77

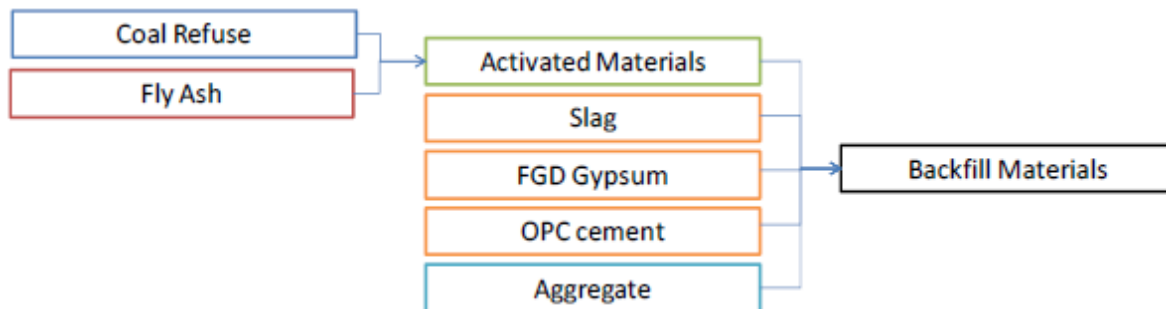


Figure 4.4.3 Scheme chart of the backfill material design (Coal refuse backfill)

Figures 4.4.4 (a) and (b) depict the flowability of the backfill material at different pulp densities. The fly ash-based backfill material had better flowability than the coal refuse-based backfill material at the same pulp density. For example, when the pulp density was 70%, the spread of the 20°C coal refuse-based backfill material was 201 mm, whereas that of the 20°C fly ash-based backfill material was 301 mm. The various contents of the thermal-activated material showed different flowability patterns, and thermal activation from 20°C to 950°C significantly increased the flowability of the coal refuse-based backfill material. However, the flowability of the fly ash-based backfill material began to decrease when the activation temperature exceeded 550°C.

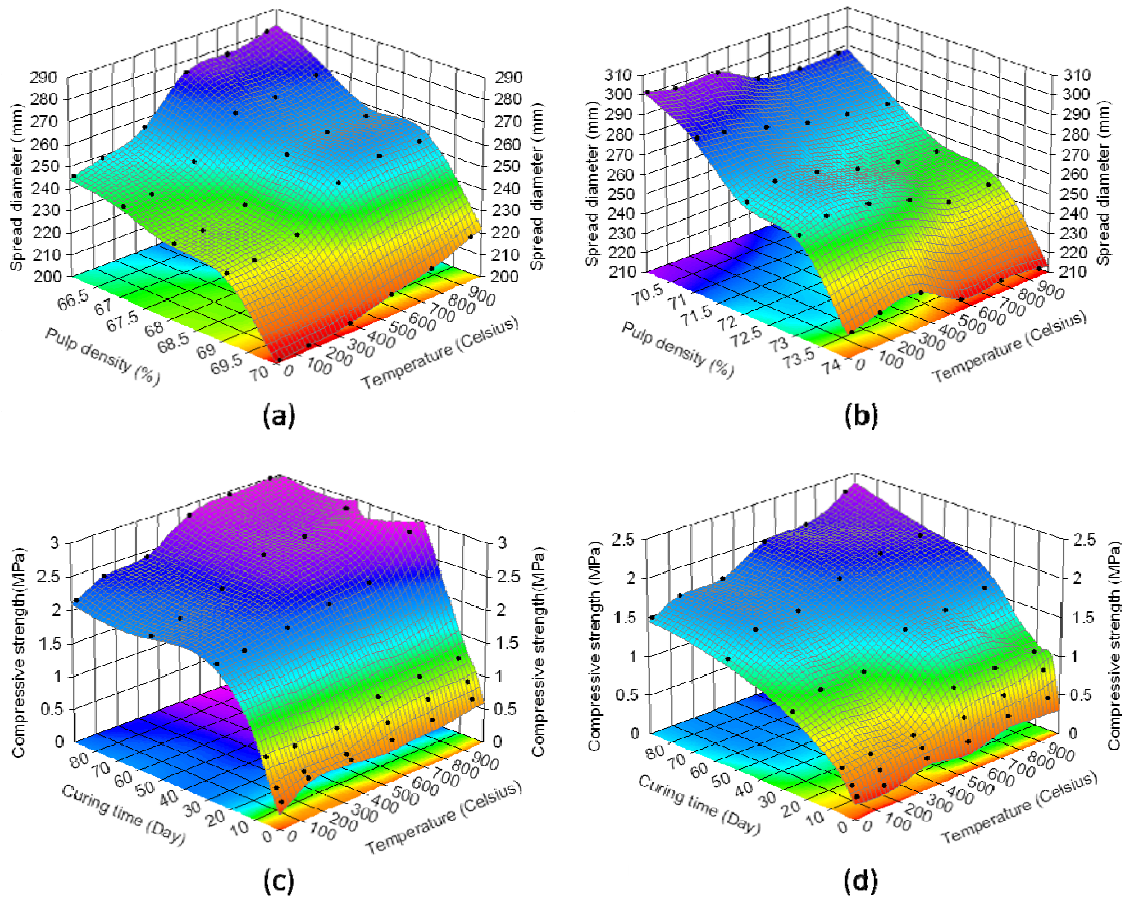


Figure 4.4.4 Performance of the backfill material

(a) Flowability of the coal refuse-based backfill material; (b) Flowability of fly ash-based backfill material; (c) Compressive strength of the coal refuse-based backfill material; (d) Compressive strength of the coal refuse-based backfill material.

(Each black point on figure 4 (a) and (b) represents the mean of 6 replicates at one recipe design, and none of the standard deviation in recipe design is larger than 2.5; Each black point on figure 4(c) and (d) represents the mean of 12 replicates at one recipe design, and none of the standard deviation in recipe design is larger than 0.02)

Unconfined compressive strength is another important factor to evaluate the performance of backfill material. Figures 4.4.4 (c) and (d) show the compressive strength measured at six different curing times (1, 3, 7, 28, 56 and 90 days) at a pulp density of 70%. It was found that the activated coal refuse-based backfill material had a higher unconfined compressive strength than that of the fly ash-based backfill material, indicating that the activated coal refuse has better pozzolanic properties than the activated fly ash. Thermal activation from 20°C to 950°C increased the pozzolanic property of the activated coal refuse, which had better pozzolanic property than the activated fly ash at the same activation temperature, especially for the 90 days cured sample. For instance, the 750°C coal refuse-based backfill material had an unconfined compressive strength of 2.94 MPa after 90 days of curing, while the 950°C coal refuse-based backfill material had 2.98 MPa at the same curing condition. The 750 °C fly ash-based backfill material had an unconfined compressive strength of 2.02 MPa at 90 days, and the 950 °C fly ash-based backfill material reached 2.31 MPa.

#### 4.4.5. Optimal design of backfill material.

As mentioned above, thermal activation improved the pozzolanic properties and the flowability of the coal refuse; however, the thermal activation process did not help much for the fly ash to gain better pozzolanic properties, and instead it resulted in decreased flowability caused by fly ash agglomeration beyond 550°C. Considering the economic and environmental factors, the optimal design was achieved when combining the advantages of the 750°C coal refuse and 20°C fly ash without activation which had better flowability than the lower temperature (below 550°C) activated coal refuse for the backfill slurry. Table 4.4.2 lists the composition of Backfill Material Group B (B1 to B5), which can be used to determine the optimal design for the backfill material with a mixture of 750°C coal refuse and 20°C fly ash.

Table 4.4.2 Composition of Backfill Material Group B

	Binder			Activated material		Aggregate
	Cement	Slag	FGD gypsum	750°C Coal refuse	20°C Fly ash	Coarse Refuse
B1% (w/w)	1	1	1	20	0	77
B2% (w/w)	1	1	1	15	5	77
B3% (w/w)	1	1	1	10	10	77
<b>B4% (w/w)</b>	<b>1</b>	<b>1</b>	<b>1</b>	<b>5</b>	<b>15</b>	<b>77</b>
B5% (w/w)	1	1	1	0	20	77

Figure 4.4.5 illustrates the flowability tests of B1 to B5. These tests indicated that increasing the content of the 20°C fly ash greatly improved the flowability of the fresh slurry. According to backfill work experience, ACI regulations, a range between 200 and 300 mm is acceptable for mining backfill applications (ACI 229R, 1999). B4 (5% 750°C coal refuse + 15% 20°C fly ash) is an optimal design for flowability because most of the spread fell within 200-300 mm when the pulp density was shifted from 70% to 75%. Although B5 (0% 750°C coal refuse + 20% 20°C fly ash) had slightly better flowability than B4, B5 is not a good choice when bleeding and compressive strength are considered. High content fly ash-based backfill material has a bleeding problem because of the spherical ball shape of the fly ash. The 5% coal refuse has better water absorption ability when compared with the same amount of fly ash.

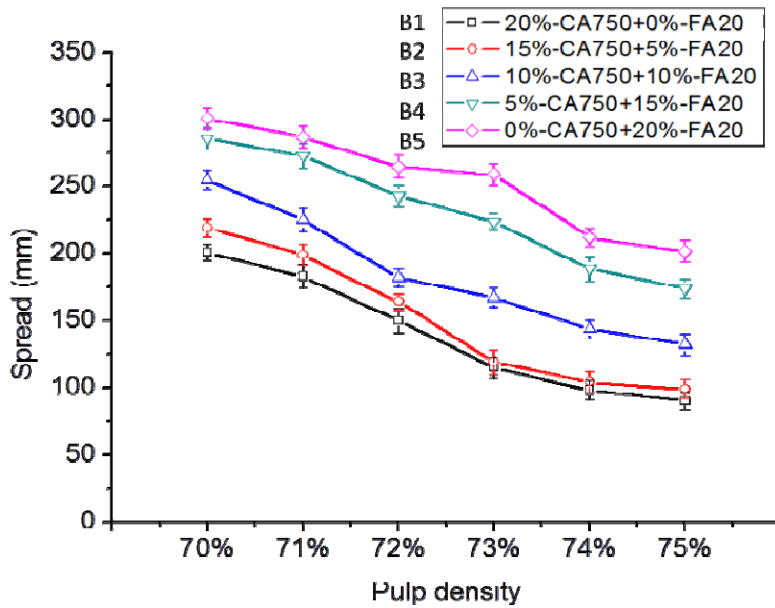


Figure 4.4.5 Flowability test of Backfill Material Group B

Table 4.4.3 illustrates the bleeding rate of B1 to B5 at a pulp density of 73%. The increased amount of coal refuse reduced the bleeding rate. The bleeding rate difference between B4 (3.29%) and B5 (6.07%) was significant. Figure 4.4.6 shows that the compressive strength of B4 at a pulp density of 73% met the target compressive strength requirements for 28 days (1 MPa) for the backfill industry (Sun et al., 2004); the 28 day strength was 1.4 MPa, and the 90 day strength was 2.7 MPa.

Table 4.4.3 Bleeding rates of B1-B5

	B1	B2	B3	B4	B5
Bleeding rate (%)	2.45	2.87	3.01	3.29	6.07

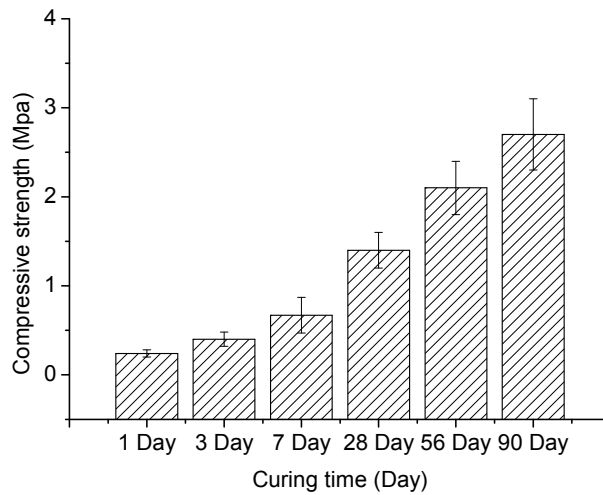


Figure 4.4.6 Compressive strength test of Backfill Material Group B4

#### 4.4.6. TCLP Results

The main environmental concern about the utilization of coal refuse, fly ash, and final products is the possibility that certain constituents in these wastes may leach into the groundwater at concentrations determined to be potentially hazardous to human health. However, the TCLP results of the raw fly ash, raw coal refuse and 180 day backfill hydration products B4 are shown in Table 4.4.4 and reveal that none of the metals leaching levels exceeded the EPA limitations. These results indicate that the backfill material is environmentally acceptable. There was also no significant difference in the leaching results between the raw coal refuse and the 750°C activated coal refuse. Although some studies have been recently published on the relevant role of organic carbon on metal leaching (Ludwig et al., 2002; Brown et al., 2003), the total effect of organic carbon on metals leaching from the backfill material was not significant in this test. The mechanism of formation of organic carbon-heavy metal complexes and the related molecular modeling require further investigation.

#### 4.4.7. Comparison with Other Backfill Materials

Backfill industry involves different factors which might influence the final application, such as backfill material, location of mine, geometry of the underground space, transportation facilities, etc. The performance and requirement of backfill material varies from mine to mine. Although each of these backfill methods has some unique characteristics, they share some disadvantages when using largely Ordinary Portland cement as the binder. These disadvantages include the following aspects. 1) A large amount of cement in the slurry is carried away by water during the dewatering process, which not only causes environmental problems but also decreases the strength of the backfill body. 2) Only the coarse fractions of the tailings can be used as aggregate

to create high permeability in the backfill body. The utilization efficiency of the tailing is less than 40%. The large quantity of unused fine tailings must be disposed of, which causes environmental problems on mine surfaces; 3) The purchase of sands to create aggregates is costly if the amount of tailings available is not sufficient for backfill.

Table 4.4.4 TCLP results (Backfill body)

Constituent	Raw Fly ash (ppm)	Raw Coal refuse (ppm)	750 Coal refuse (ppm)	B4 180 day Backfill sample (ppm)	EPA Limits (ppm)
Antimony	0.37	<0.05	<0.05	<0.05	-
Arsenic	<0.05	<0.05	<0.05	<0.05	5.0
Barium	0.91	0.547	0.598	0.207	100.0
Beryllium	<0.025	<0.025	<0.025	<0.025	-
Cadmium	<0.025	<0.025	<0.025	<0.025	1.0
Chromium	0.15	<0.05	<0.05	<0.05	5.0
Cobalt	0.10	<0.01	0.0116	<0.01	-
Copper	<0.01	<0.01	0.0133	<0.01	-
Lead	<0.05	<0.05	<0.05	<0.05	5.0
Mercury	<0.0001	<0.0001	<0.0001	<0.0001	0.5
Molybdenum	<0.01	<0.01	<0.01	<0.01	-
Selenium	<0.01	<0.01	<0.01	<0.01	1.0
Silver	<0.05	<0.05	<0.05	<0.05	5.0
Thallium	<0.05	<0.05	<0.05	<0.05	-
Vanadium	<0.01	<0.01	<0.01	<0.01	-
Zinc	<0.01	<0.01	0.0242	<0.01	-

Alternatively, the developed silica-alumina backfill material was used to easily control the pulp density of the backfill slurry at 70-75%, which provided high flowability and a low bleeding rate. This developed technology can use mining waste-coal refuse as coarse aggregates and provide a huge economic benefit to industry. Along with 1% of OPC dosage, all materials used in this backfill technology are from industrial waste resources, which mean this backfill technology significantly reduces the cost of the industrial input. The major concern for this technology is energy and time input for the coal refuse thermal activation process. However, the coal refuse activated in 45 minutes should be acceptable for backfill application based on the activation process input. Additionally, thermal activated coal refuse accounts for only 5% of the total solid materials, which means only a small amount of energy is consumed. Furthermore, the remainder of the thermal activated coal refuse is successfully used to produce coal refuse blended cement. In this case, the binary utilization of the thermal activated coal refuse makes this technology more realistic when considering economic factors. Table 4.4.5 describes the advantages of this silica-alumina-based backfill material over the traditional backfill material.

Table 4.4.5 Technical index of the backfill technology

Technical index	Hydraulic /Rock Backfill	Paste Backfill	Silica alumina coal refuse based Backfill
Binder	Cement	Cement	Cement, slag and gypsum
Aggregate	Coarse to medium course sand, rock	Graded tailings, total tailing, river sand	Coal refuse, fly ash, other industry wastes
Pulp Density	55-70%	75-85%	70-75%
Flowability	Good	Poor	Good
Transportation	By gravity	Using high pressure pump	By gravity or using low pressure pump
Capital investment	Relatively Low	High	Relatively Low
Filling capability	>100 m <sup>3</sup> /h	30-50 m <sup>3</sup> /h	>100 m <sup>3</sup> /h
Processing	Complicated	Difficult	Relatively easy
Evaluation	Dewatering Low strength	No dewatering Relative high strength	No dewatering Relative high strength

In conclusion, the backfill technology described in this section is typically a solution for utilizing a large amount of coal refuse from West Virginia, it can be referred as a solution for various mine conditions by adjusting the present method of producing the material and its composition and by adjusting the production method for new backfill slurry and its transportation procedures.

## 5. Benefits Assessment

### 5.1. Preparation and Performance of Green Cement-Coal Refuse Based Cementitious Material (CRC)

Due to different substitute portion of coal refuse save different amount of energy, we take an optimal recipe according to the previous experiment completed in Chapter 3. And an energy calculation is provided to illustrate the energy saving benefit based on this optimal recipe.

All tests were performed according to the provisions of the relevant American Society for Testing and Materials (ASTM) standards as listed in Table 5.1. The recipe designs of different cementitious materials and the mixture proportions of concrete are described in Table 5.2. The mixing strictly followed ASTM C109. The proportion of materials for the standard mortar was one part of cement to 2.75 parts of graded standard sand by weight and the W/C (water/cementitious material) ratio was controlled as 0.485. And superplasticizer with amount of 1.0% of the total weight of CRC group was added to adjust the flowability of the cementitious material.

Table 5.1 ASTM standards on the performance tests

Compressive strength of hydraulic cement mortars	ASTM C109
Flow of hydraulic cement mortar	ASTM C1437
Fineness of hydraulic cement by air-permeability apparatus	ASTM C204
Density of hydraulic cement	ASTM C188
Time of setting of hydraulic cement by Vicat needle	ASTM C191
Standard specification for blended hydraulic cements	ASTM C595
Standard Performance Specification for hydraulic Cement	ASTM C1157

Table 5.2 Mixture composition of the cementitious material

	Cement (%)	Coal refuse (%)	Slag (%)	Gypsum (%)
CRC	30	50	16.5	3.5
OPC	100	0	0	0

Note: CRC=Coal refuse based cementitious material; OPC=Ordinary Portland cement

From Table 5.3, it was clearly seen that the performance of CRC satisfies the ASTM requirement. For example, although the setting time of CRC was longer than that of OPC, it still met with the requirement of ASTM C150 (Initial  $\geq 45$ min; Final  $\leq 375$  min). Its consistency of CRC mortar tested by a standard flow table reached to 106 (requirement of 105-115 in the case of ASTM C109), which means the flowability of the mortar paste in the experiment is acceptable. As for the compressive strength, it performed very well to meet with all the requirements in ASTM

C595 and ASTM C1157, and CRC had an even higher compressive strength in 28 curing day than that of OPC control group. According to the ASTM 1157 requirement, the compressive strength needs to reach not less than 10 MPa on 3 days and not less than 17 MPa on 7 days. Therefore, this designed green cement CRC met with the ASTM standards very well in this experiment.

Table 5.3 Physical and Mechanical Performance of CRC and OPC

	Specific gravity (kg/m <sup>3</sup> )	Specific surface (m <sup>2</sup> /kg)	Setting time (min)		Compressive Strength (MPa)				Flow
			Initial	Final	1 D	3 D	7 D	28D	
CRC	2.90	467	161	258	10.2	26.2	32.0	47.7	106
OPC	3.01	425	145	202	11.6	27.3	33.4	45.2	111

## 5.2. Energy consumption calculation for OPC production

Based on the data of 2001-2010, the energy consumption in OPC production is approximately 5.02MBtu/ton of cement, which includes the quarrying energy (Choate, 2003). The detail energy usage for each procedure from quarrying/crushing, raw grinding, kiln processing to finish milling is illustrated below.

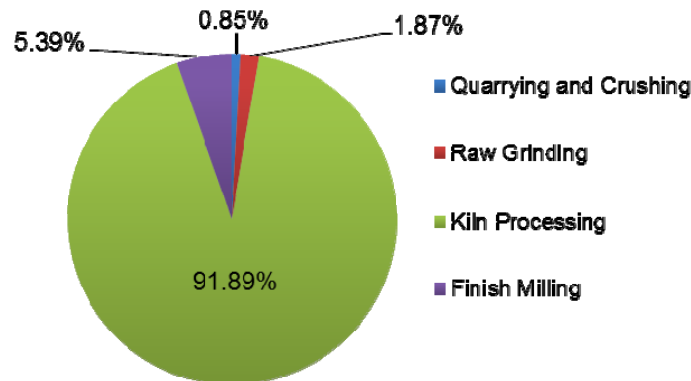


Figure 5.1 Energy consumption in cement production (Based on the data Choate W, 2003)

Generally, the whole production of cement production can be divided into three stages as the following: (1) Process one, including quarrying, crushing and raw grinding, consumes approximately 0.14 MBtu/ton (0.33<sup>P</sup> MBtu/ton); (2) Process two, including pyro-processing, consumes approximately 4.61 MBtu/ton (96.3% fuel and 3.7% electricity, 4.94<sup>P</sup> MBtu/ton); (3) Process three, including finish milling and mixing, consumes approximately 0.27 MBtu/ton (0.79<sup>P</sup> MBtu/ton). In the following calculation, the energy consumption in green cement-coal

refuse based cementitious material production was compared with that in traditional OPC production on each specific process.

Note: primary energy accounts for the fact that substantial electrical generation inefficiencies and transmission losses occurring outside the cement manufacturing facility. Typical U.S. grid electricity requires about 9,935 Btu of energy to deliver 1kwh of on-site electricity (3,413 Btu). Hence, the primary energy is the total energy of fuels which are directly used in the cement manufacturing and used to generate and deliver on-site electricity. The formula can be modeled as Primary Energy (represent as <sup>P</sup> MBtu/ton) = Fuel energy × Correction Factor (CF) + 3 × On-site Electricity Energy, (CF=1.14). The correction factor is derived from the calibration of fuel energy consumption data in 2001 with the data reported by William T. Choate in 2002 (Choate, 2003.)

### 5.3. Comparison of energy consumption between ordinary Portland cement production and green cement-coal refuse based cementitious material production.

Figure 5.2 shows a comparison between the ordinary Portland cement production and green cement-coal refuse based cementitious material production. The energy consumption for producing one ton of coal refuse based cementitious material cement is 2.7 MBtu/ton (3.20 <sup>P</sup>MBtu/ton) less than that for ordinary Portland cement production. For the mathematic calculation, 1 unit of cement is made from 0.9 unit of clinker and 1.43 unit of limestone, 1 unit of coal refuse produces 0.9 unit of pozzolana in this experiment.

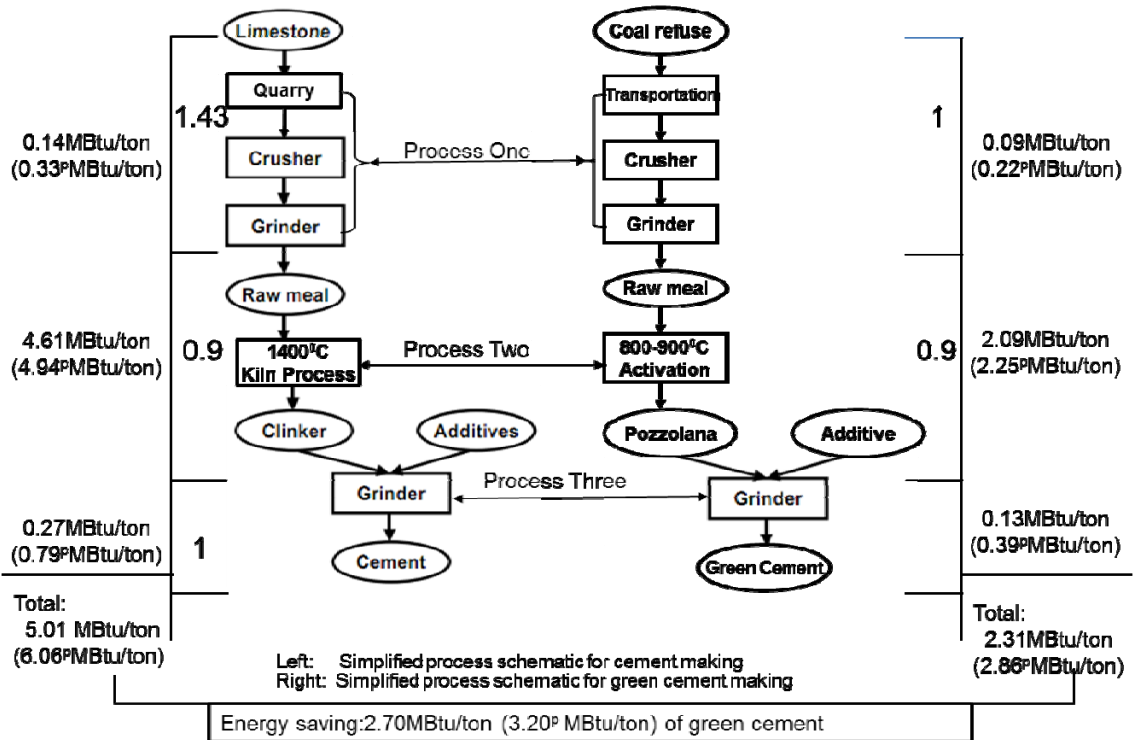


Figure 5.2 Energy consumption comparisons between green cement and ordinary Portland cement

### 5.3.1. Detailed Calculation for Process One

Figure 5.3 illustrates the calculation summary of green cement production in process one. The production of green cement only costs 16,897 Btu/ton in this process. Compared with traditional OPC production, the energy saving of green cement is 0.05 Mbtu/ton. Unlike limestone and cement rock, coal refuse as stockpiled solid waste does not need quarrying, which eliminates the energy consumption of pumps, percussion drill and water tanker for acquiring raw materials. According to the statistic data from 2001 to 2010, the energy consumption for quarrying and transporting one ton of limestone and cement rock is approximate 37.833Btu/ton (Choate, 2003). It means by using coal refuse as raw material could saves a lot of energy from quarrying and transportation during process one. On the other hand, except 50% pozzolana (one unit of raw coal refuse produces 0.9 unit of pozzolana after thermal activation) and 30% cement, the rest majority part of the green cement are from the industry solid waste, which means that it does not need quarrying energy input. The energy consumption of green cement on the quarry stage is 0.021MBtu/ton, and the calculation is as following:

(a) Energy for quarrying one ton of pozzolana:  
 $16,897 \text{ Btu/ton of coal refuse} / 0.9 = 18,774.4 \text{ Btu/ton of pozzolana (0.02}^{\text{P}}\text{MBtu/ton)}$

(b) Energy for quarrying one ton of green cement:  
 $18,774.4 \times 0.5 + 0.3 \times 37,833 \text{ Btu/ton} = 0.021 \text{ MBtu/ton of green cement (0.024}^{\text{P}}\text{MBtu/ton)}$

In the laboratory practice, the raw coal refuse is ground by lab ball mill to reduce its size for passing 200-Mesh screen whose size is good for thermal activation in the laboratory scale experiment. In the cement industry, the raw materials are ground to 70-80% of original size for passing 200-Mesh screen. Considering the similar hardness of coal refuse and limestone, the minor difference of grinding energy input between coal refuse and limestone is not accounted in the calculation. In this case, energy for crushing and grinding one ton of limestone (rock) equals to energy for crushing and grinding one ton of coal refuse (rock). The calculation on the energy consumption for crushing and grinding stage is as following:

(a) Energy for crushing one ton of limestone:  
 $0.0035 \text{ MBtu/ton (0.010}^{\text{P}}\text{MBtu/ton)}$

Energy for crushing one ton of green cement:

$0.0035 \text{ MBtu/ton of coal refuse} = 0.0039 \text{ MBtu/ton (0.01}^{\text{P}}\text{MBtu) of pozzolana}$

$0.0039 \times 0.5 + 0.005 \times 0.3 = 0.0034 \text{ MBtu/ton (0.01}^{\text{P}}\text{MBtu) of green cement}$

(b) Energy for grinding one ton of limestone:  
 $0.063 \text{ MBtu/ton (0.189}^{\text{P}}\text{MBtu/ton) of limestone}$

Energy for grinding one ton of green cement:

0.063MBtu/ton of coal refuse=0.07MBtu/ton (0.21<sup>P</sup>MBtu/ton) of pozzolana

$0.07 \times 0.5 + 0.09 \times 0.3 = 0.062 \text{MBtu/ton}$  (0.19<sup>P</sup>MBtu/ton) of green cement

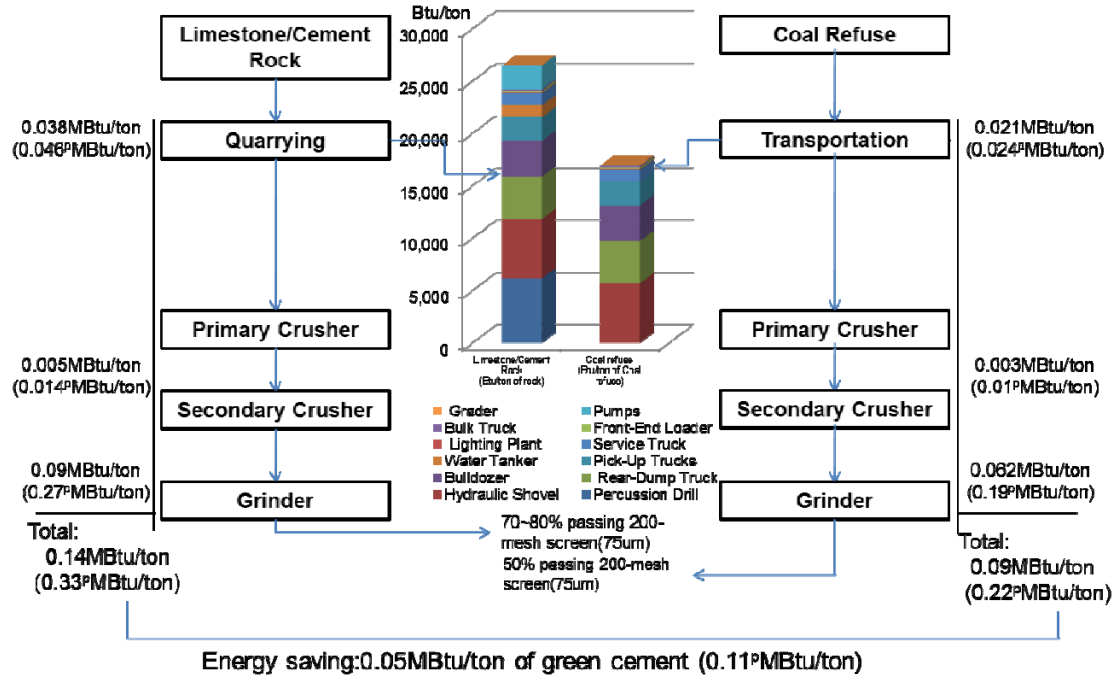


Figure 5.3 On-site and primary energy consumption by cement making and green cement making in Process one

### 5.3.2. Detailed Calculation for Processing Two.

Figure 5.4 shows the summary of calculation for process two. It is shown that there are four major components in this process: (a) Heat requirement for chemical reactions; (b) Heat loss; (c) Energy from coal refuse; (d) Evaporation of water. Basically, in this process, there are two major factors causing energy saving. The first one is relative “low temperature” heating process which only requires heating at 700-800°C which is significantly lower than the 1200°C-1540°C of the OPC manufacturing. The second factor is the combustion part in the coal refuse which contributes 0.4Mbtu/ton because of the internal combustion during this heating process. It saves the energy cost from the external energy resources. Therefore, the calculated result of the energy cost of pozzolana production is only 2.09Mbtu/ton, which is much lower than the 4.61Mbtu/ton of the clinker production.

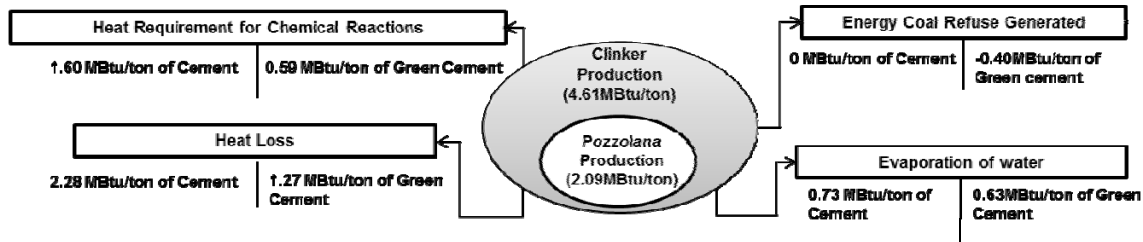


Figure 5.4 Energy consumption summary of green cement production in process two

### 5.3.3. Detailed Estimation for Process Three.

In cement industry, energy consumption from electricity for making OPC final product is about 0.27MBtu/ton of cement (0.79<sup>p</sup>MBtu/ton) (Choate, 2003). In our work, the experiment was designed to estimate the electricity consumption through grinding OPC into higher specific surfaces. The type I/II cement was processed with the same procedures for one and two hours respectively as calculation samples. The specific surface changes as time prolonged are given below.

Table 5.4 Relationship between specific surface and grinding time

	Original Specific Surface (cm <sup>2</sup> /g)	After 1hr's milling	After 2hr's milling
OPC	3818.00	4745.00	5205.00

For OPC grinding process, the energy consumption is approximate 0.1MBtu/ton (0.3<sup>p</sup>MBtu/ton) of cement for increasing its specific surface from 3818 to 5205 cm<sup>2</sup>/g (see Table 5.4), which is equal to the amount of energy consumption for grinding the pozzolanic material based on our lab experiments. Therefore, the energy consumption in the final grinding for the coal refuse based green cement is  $0.5 \times 0.1 + 0.3 \times 0.27 = 0.13$ MBtu/ton (0.39<sup>p</sup>MBtu/ton) with this process.

### 5.4. CO<sub>2</sub> Emission Calculation

The coal refuse thermal activation is controlled at 700-800°C which is significantly lower than the 1200°C -1540°C of the OPC manufacturing. The majority CO<sub>2</sub> emission is decomposed from the Calcite of the limestone at the temperature around 800-900°C, which is higher than the temperature (700-800°C) for the coal refuse thermal activation. Principally, the manufacturing of the coal refuse based green cement does not generate CO<sub>2</sub> from raw materials decomposition during the thermal activation process. Figure 5.5 illustrates the CO<sub>2</sub> emission comparison between the OPC and CRC.

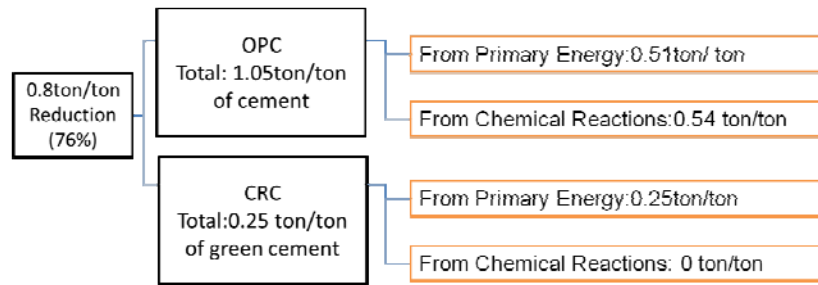


Figure 5.5 CO<sub>2</sub> emission comparisons between OPC and CRC

### 5.5. Summarization of the potential energy saving and CO<sub>2</sub> emission reduction

1. Figure 5.2 indicates that the overall energy saving estimated for the coal refuse based green cement production compared with OPC production is about 54% (( 5.01MBtu/ton- 2.31MBtu/ton)/5.01MBtu/ton=54%).
2. Figure 5.5 indicates that the overall CO<sub>2</sub> reduction estimated is about 76% ((1.05ton/ton- 0.25ton/ton)/1.05ton/ton=76%).

## **6. Commercialization**

This project is a TRL 1 research stage which provides the scientific feasibility of a technology for future commercialization to improve the energy efficiency and reduce the greenhouse gas emission but it does not contain any approaches or planning for future commercialization.

## 7. Accomplishments

### Publications

- Y.Yao. (2012). Ph.D Dissertation. University of the Pacific. *Performance and mechanism on a high durable silica alumina based cementitious material composed of coal refuse and coal combustion byproducts.*
- Y.Yao, H.Sun. (2012). A novel silica alumina-based backfill material composed of coal refuse and fly ash. *Journal of Hazardous Materials.* 213-214:71-82.
- Y.Yao, H.Sun. (2012).Characterization of a new silica alumina-based backfill material utilizing large quantities of coal combustion byproducts. *Fuel.* 97:329-336.
- Y.Yao, H.Sun. (2012). Durability and leaching analysis of a cementitious material composed of high volume coal combustion byproducts. *Construction and Building Materials.*36:97-103.
- Y.Yao, H.Sun. (2012). Improvements on Pozzolanic Reactivity of Coal refuse by thermal activation. *Environment & Pollution.* 01(2): 33-38.
- Y.Yao, H.Sun. (2012). Performance and microanalysis of cement asphalt mortar with admixture of coal fly ash. *Journal of Material Science Research.* 01(2):193-206.
- Y.Yao, H.Sun. (2012). Characterization of a silica alumina based backfill material composed of coal combustion and byproducts and coal refuse. *Proceedings of 27<sup>th</sup> International Conference of Solid Waste Technology and Management.*376-387.

## 8. Conclusions

- Coal refuse shows different pozzolanic properties when they were activated to different time at different temperature from 500°C to 800°C. It was found that the optimal activation condition is at 700°C to 800°C from 0.5 hour to 1 hour.
- It was found that from XRD analyses for chlorite, muscovite, quartz and kaolinite were the major minerals of the raw coal refuse. During the thermal activation, the kaolinite and muscovite disappeared at 600°C to 800°C. The peaks associated with quartz were decreased at 800°C, and this mineral phase change might be the major contribution to the pozzolanic property change. Through the SEM image analysis, it was found that the coal refuse had layered scale microstructure at 500°C to 600°C, while this structure was destroyed when the temperature up to 700°C to 800°C.
- It appears that 30% to 50% of OPC production can be potentially substituted by activated coal refuse.
- For the silica-alumina backfill material, coal refuse can be largely recycled as cementitious material, besides only 1% OPC is introduced in the backfill mixture; the rest of the material is all industrial solid wastes, which offer enormous potentials for reducing the capital investment and operation cost for the backfill industry.
- A benefit assessment indicates that the production of the coal refuse based silica alumina cementitious material will lead to significant reduction (about 54%) in energy consumption with respect to OPC production, and significant reduction (about 76%) in CO<sub>2</sub> emission.

## 9. Recommendations

N/A

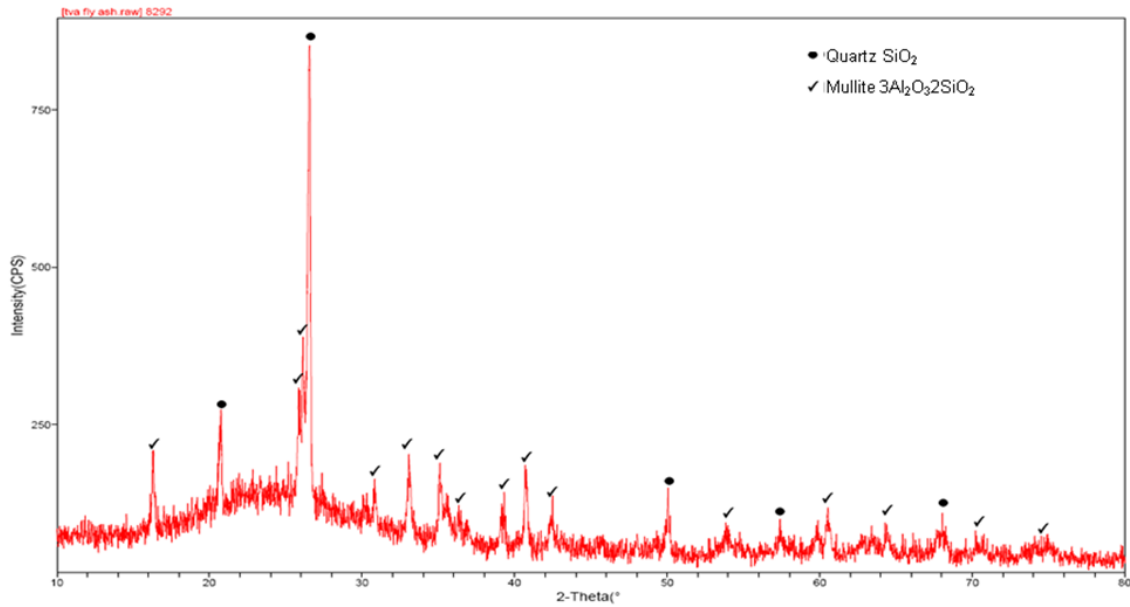
## 10. References

- [1] ACI Committee 232. (2003). *Use of fly ash in concrete (ACI 232.2R-03)*. American Concrete Institute: Farmington Hills, MI, p. 41.
- [2] ACI 229R-99 Report. (1999). *Controlled Low Strength Materials*, American Concrete Institute, Farmington Hills, MI, USA, 1999.
- [3] ASTM C109. (2008). *Standard test method for compressive strength of hydraulic cement mortar (Using 2-in. or [50-mm] cube specimens)*. Annual Book of ASTM Standards vol. 4.01, American Society for Testing and Materials, Conshohocken, PA.
- [4] ASTM C150. (2008). *Standard specification for Portland cement*. Annual Book of ASTM Standards vol. 4.01, American Society for Testing and Materials, Conshohocken, PA.
- [5] ASTM C230. (2008). *Standard specification for flow table for use in tests of hydraulic cement*. Annual Book of ASTM Standards vol. 4.01, American Society for Testing and Materials, Conshohocken, PA.
- [6] ASTM C232-07. (2008). *Standard test methods for bleeding of concrete*. American Society for Testing and Materials, Conshohocken, PA, USA 2008.
- [7] ASTM C305. (2008). *Standard practice for mechanical mixing of hydraulic cement pastes and mortars of plastic consistency*. Annual Book of ASTM Standards vol. 4.01, American Society for Testing and Materials, Conshohocken, PA.
- [8] ASTM C 595. (2008). *Standard specification for blended hydraulic cements*. Annual Book of ASTM Standards vol. 4.01, American Society for Testing and Materials, Conshohocken, PA.
- [9] ASTM C618. (2008). *Standard specification for coal fly ash and raw or calcined natural pozzolana for use in concrete*. Annual Book of ASTM Standards vol. 4.02, American Society for Testing and Materials, Conshohocken, PA.
- [10] ASTM C 666. (2008). *Standard test method for resistance of concrete to rapid freezing and thawing*. Annual Book of ASTM Standards vol. 4.02, American Society for Testing and Materials, Conshohocken, PA.
- [11] ASTM C 1157. (2008). *Standard specification for hydraulic cement*. Annual Book of ASTM Standards vol. 4.01, American Society for Testing and Materials, Conshohocken, PA.
- [12] ASTM C1202. (2008). *Standard test method for electrical indication of concrete's ability to resist chloride ion penetration*. Annual Book of ASTM Standards vol. 4.02, American Society for Testing and Materials, Conshohocken, PA.
- [13] ASTM C 1260, (2008). *Standard test method for potential alkali reactivity of aggregates (mortar-bar method)*. Annual Book of ASTM Standards vol. 4.02, American Society for Testing and Materials, Conshohocken, PA.

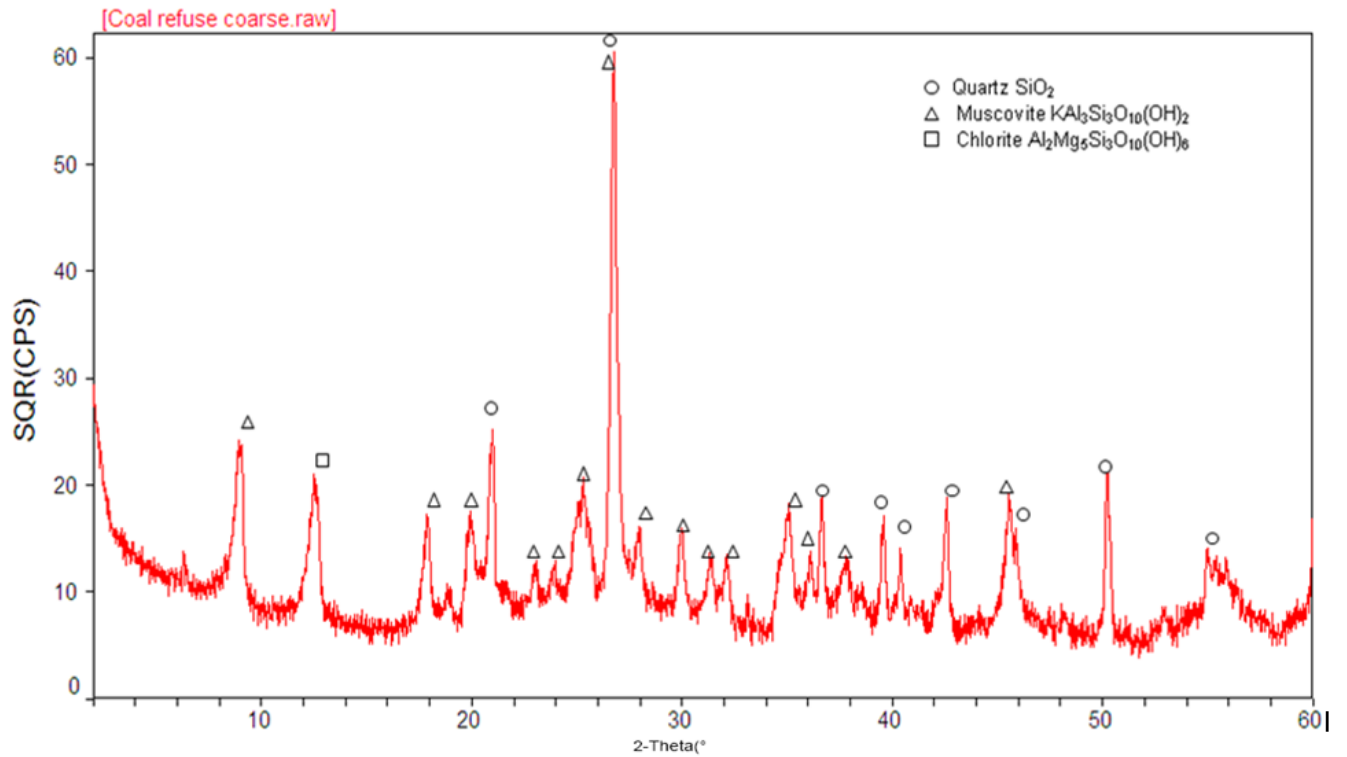
- [14] ASTM C 1567. (2008). *Standard test method for determining the potential alkali silica reactivity of combinations of cementitious materials and aggregate (accelerated mortar bar method)*. Annual Book of ASTM Standards vol. 4.02, American Society for Testing and Materials, Conshohocken, PA.
- [15] ASTM C1585. (2008). *Standard test method for measurement of rate of absorption of water by hydraulic-cement concretes*. Annual Book of ASTM Standards vol. 4.02, American Society for Testing and Materials, Conshohocken, PA.
- [16] ASTM D 6103-97. (1997). *Standard test method for flow consistency of controlled low strength material (CLSM)*. American Society for Testing and Materials, Conshohocken, PA, USA.
- [17] Brown,S., Henry,C., Chaney,R., Compton,H., DeVolder,P.Using municipal biosolids in combination with other residuals to restore metal-contaminated mining areas. *Plant and Soil*, 49 (1) (2003), 203 – 215.
- [18] CTAB. (2010). *International energy agency coal industry advisory board- 32nd plenary meeting discussion report*. OECD Headquarters in Paris.
- [19] Chatterji, S., Thaulow, N. (2000). Some fundamental aspects of alkali silica reaction. *11th International Conference on Alkali Silica Reaction*, 21-29.
- [20] Davidovits, J (2008). *Geopolymer Chemistry and Applications* (2nd ed.). Saint-Quentin, FR: Geopolymer Institute. ISBN 978-2-9514820-1-2.
- [21] Ludwig, R., McGregar,R., Blowes, D., Benner,S., Mountjoy, K.A permeable reactive barrier for treatment of heavy metals *Ground Water*, 40 (1) (2002), 59 – 66.
- [22] Yao, Y., Sun, H.H. (2012). A novel silica alumina-based backfill material composed of coal refuse and fly ash. *Journal of Hazardous Materials*, 213-214, 71-82.
- [23] Yao, Y., Sun, H.H. (2012). Characterization of a new silica alumina-based backfill material utilizing large quantities of coal combustion byproducts. *Fuel*, 97, 329-336.
- [24] Zhang, C., Yang, X., Li, Y. (2012). Mechanism and structural analysis of the thermal activation of coal-gangue. *Advanced Material Research*, 356-360, 1807-1812.
- [25] Zhang, N., Sun, H.H., Liu, X.M., Zhang, J.X. (2009).Early-age characteristics of red mud-coal gangue cementitious material. *Journal of Hazardous Materials*, 167 (1-3), 927-932.
- [26] Zhang, N., Liu, X.M., Sun, H.H., Li, L.T. (2011a). Evaluation of blends bauxite-calcination-method red mud with other industrial wastes as a cementitious material: Properties and hydration characteristics. *Journal of Hazardous Materials*, 185(1), 329-335.

# 11. Appendix

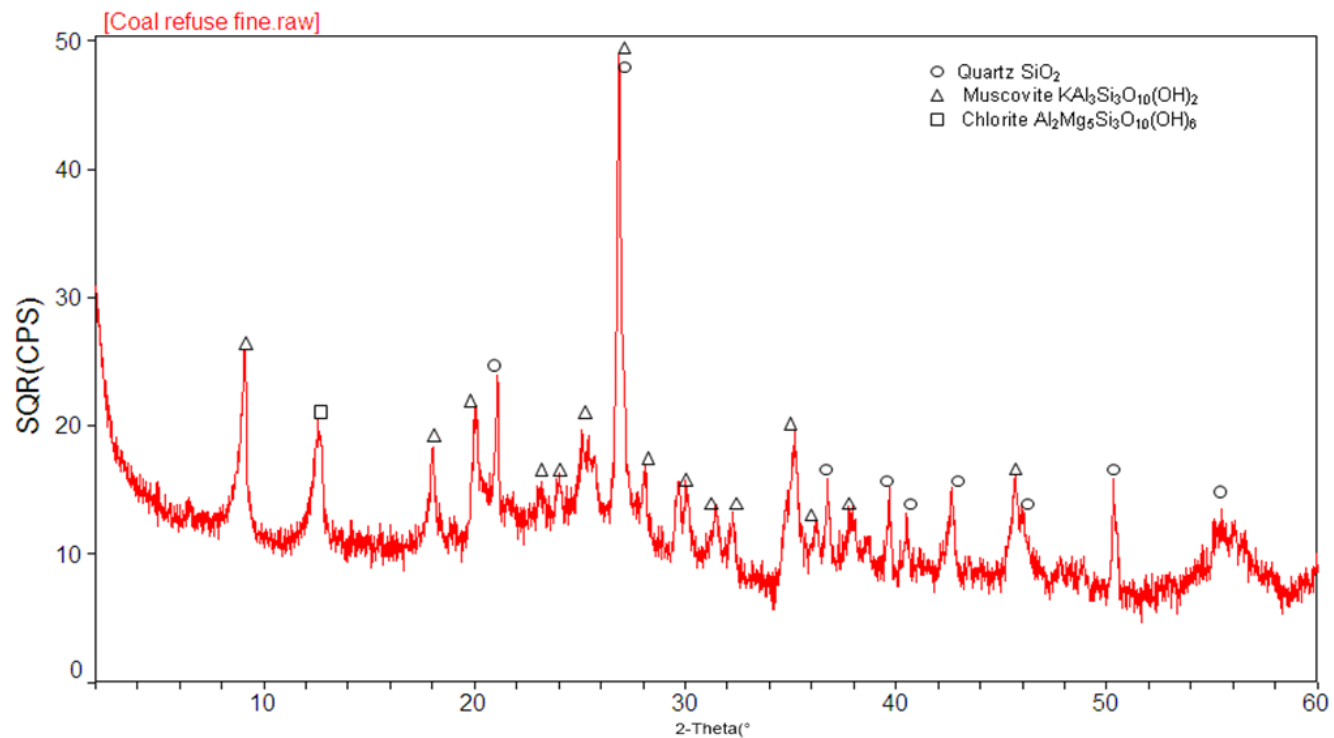
## XRD Results and Interpretation



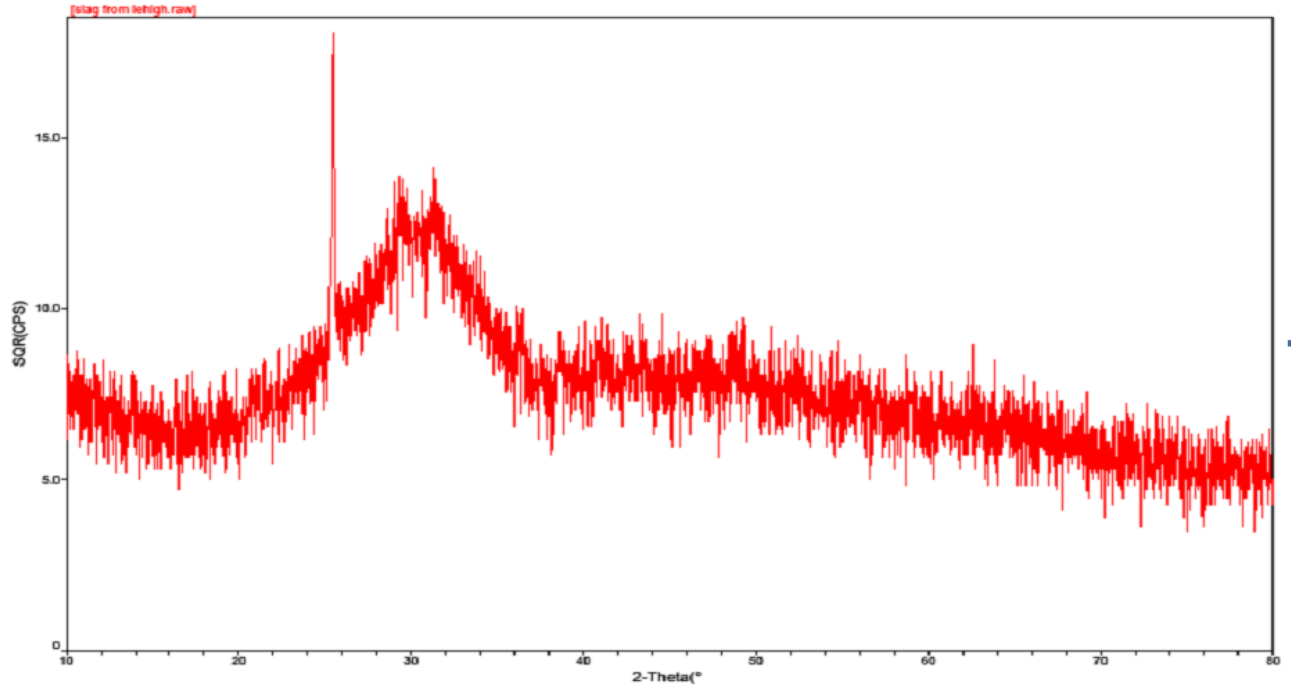
The fly ash was supplied by Tennessee Valley Authority (TVA), TN. The hump in the  $2\theta$  range from  $20^\circ$ - $34^\circ$  represents the existence of amorphous phase. The crystal phases contain mainly Quartz ( $\text{SiO}_2$ ) and Mullite ( $3\text{Al}_2\text{O}_3\cdot 2\text{SiO}_2$ ).



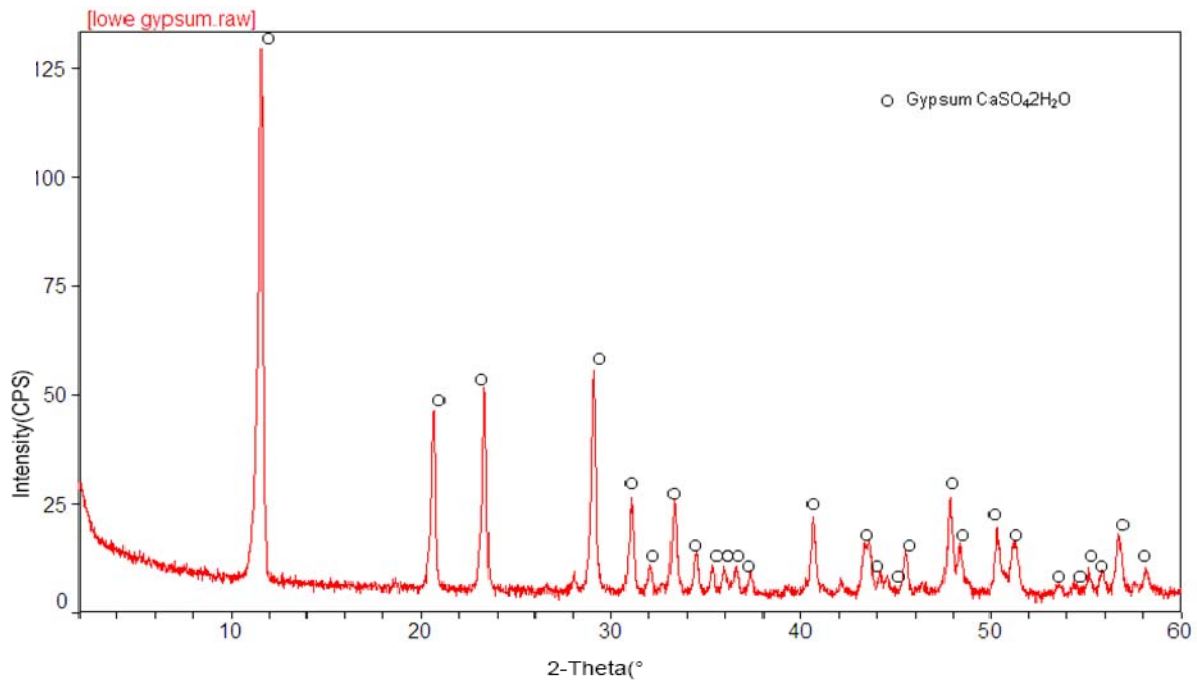
Coal refuse was provided by Arch Coal, West Virginia. There is Chlorite (Al<sub>2</sub>Mg<sub>5</sub>Si<sub>3</sub>O<sub>10</sub>(OH)<sub>6</sub>), Muscovite (KAl<sub>3</sub>Si<sub>3</sub>O<sub>10</sub>(OH)<sub>2</sub>) and Quartz (SiO<sub>2</sub>) existing in the coal refuse.



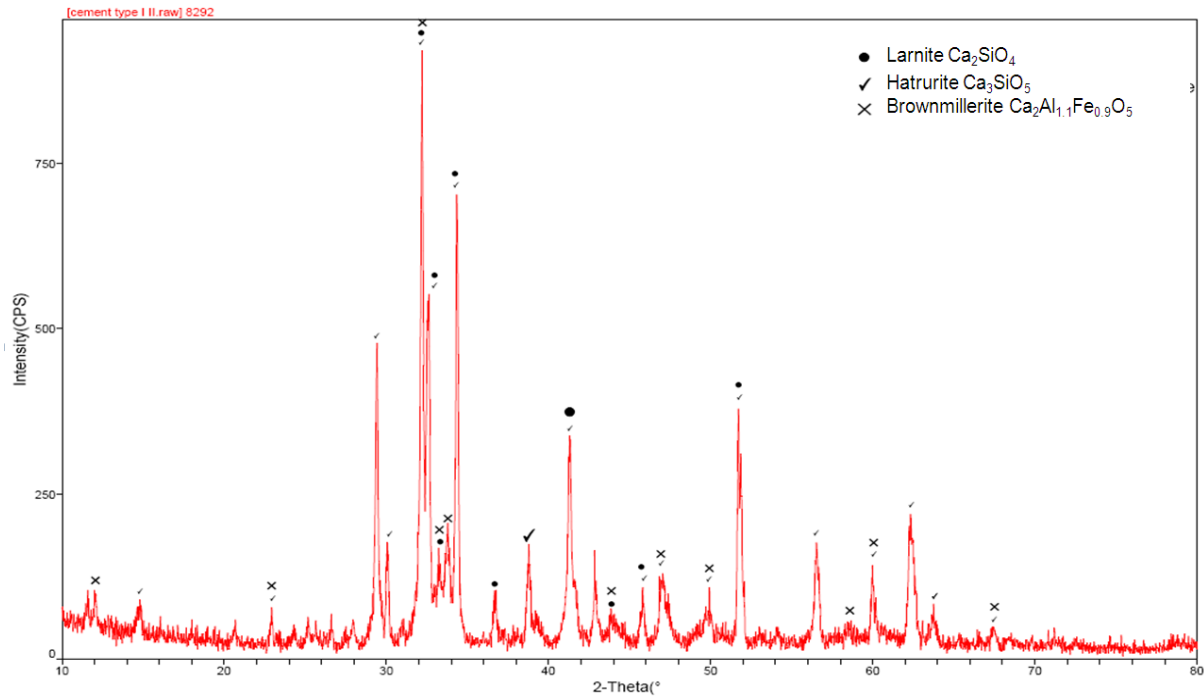
Coal sludge (dry) was provided by Arch Coal, West Virginia. There is Chlorite (Al<sub>2</sub>Mg<sub>5</sub>Si<sub>3</sub>O<sub>10</sub>(OH)<sub>6</sub>), Muscovite (KAl<sub>3</sub>Si<sub>3</sub>O<sub>10</sub>(OH)<sub>2</sub>) and Quartz (SiO<sub>2</sub>) existing in the coal sludge.



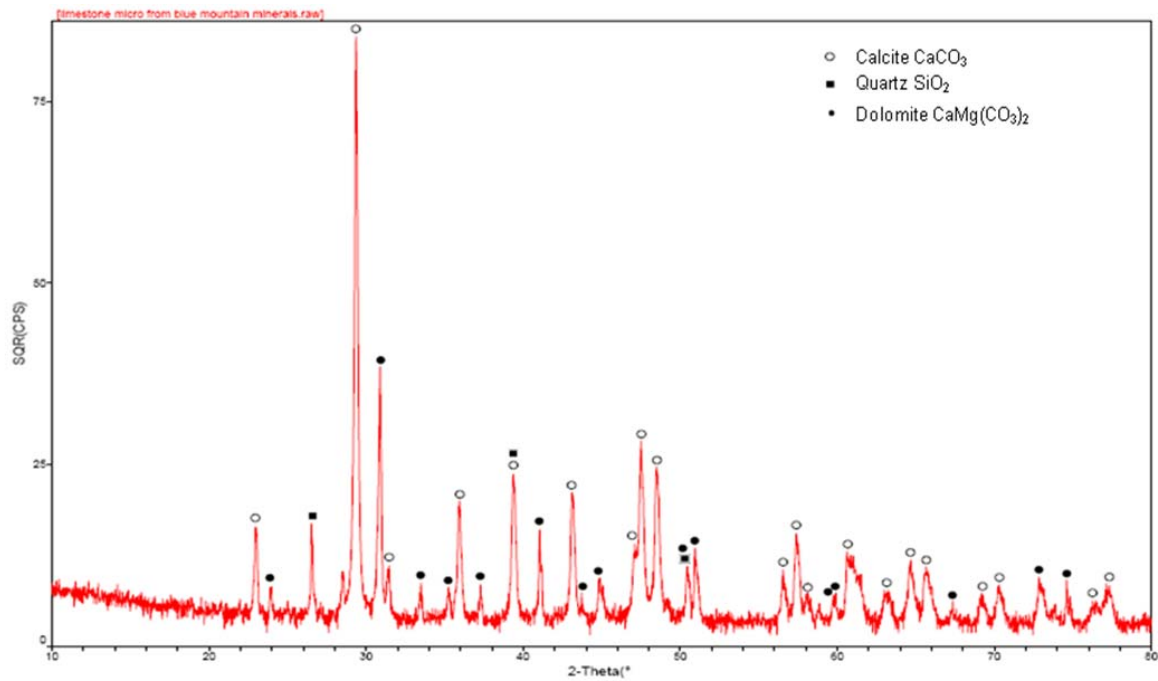
The slag is supplied by Lehigh, Stockton port terminal, Stockton, CA. Based on the XRD result, the main phase of slag is amorphous, due to the huge hump ranging from 10-80°. The single peak at 26° could be hardly interpreted.



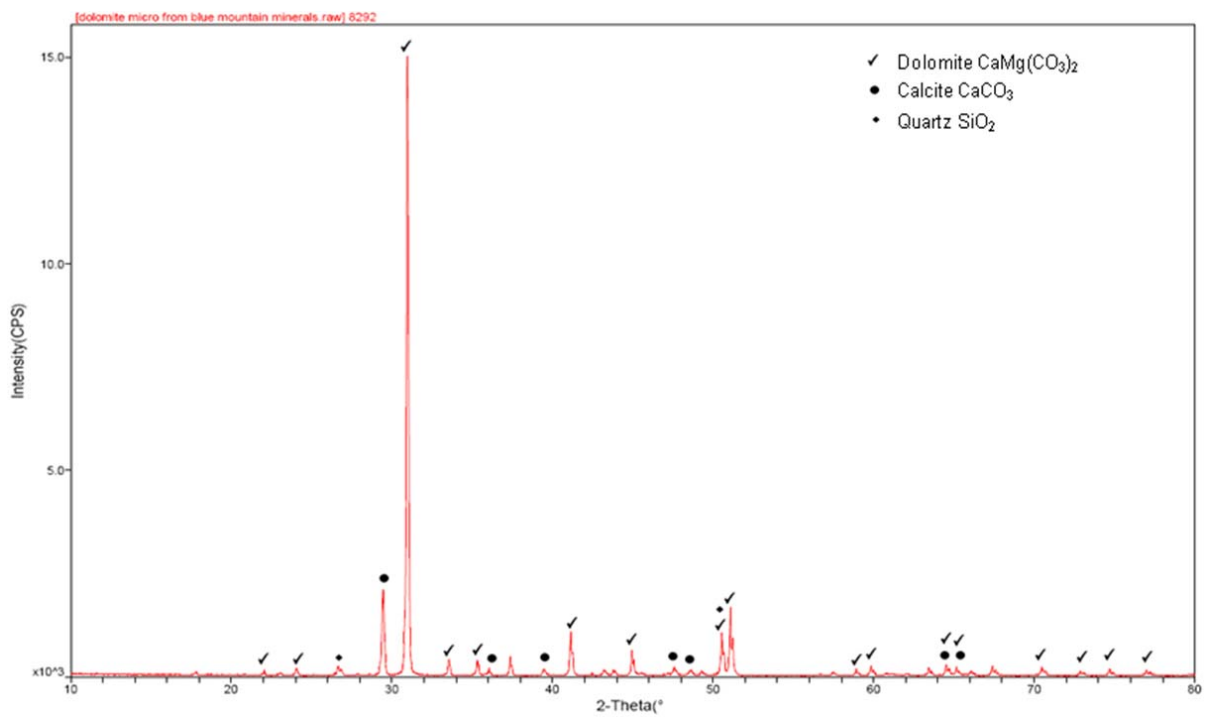
Gypsum is purchased from Lowe's store. The composition of gypsum is almost pure  $\text{CaSO}_4 \cdot 2\text{H}_2\text{O}$ .



Cement Type I/II was purchased from local Lowe's store in Stockton, CA. It is composed mainly of crystal phases which are Larnite, Hatrurite and Brownmillerite.



Limestone was supplied by Blue Mountain Minerals, Stockton, CA. The XRD result shows the main phase is Calcite ( $\text{CaCO}_3$ ) with partially Dolomite ( $\text{CaMg}(\text{CO}_3)_2$ ) and minor Quartz ( $\text{SiO}_2$ ).



Dolomite was supplied by Blue Mountain Minerals, Stockton, CA. Based on XRD results, the main phase is crystal Dolomite ( $\text{CaMg}(\text{CO}_3)_2$ ). Except from the dominant Dolomite phase, the existence of Calcite ( $\text{CaCO}_3$ ) and minor Quartz ( $\text{SiO}_2$ ) are also found.